L. F. Agnati, K. Fuxe, C. Nicholson and E. Syková (Eds.)
Progress in Brain Research, Vol 125

CHAPTER 6

Extracellular space diffusion and pathological states

Eva Syková*, Tomáš Mazel, Lýdia Vargová, Ivan Voříšek and Šárka Prokopová-Kubinová

Department of Neuroscience, 2nd Medical Faculty, Charles University and Institute of Experimental Medicine, Academy of Sciences of the Czech Republic, Vídeňská 1083, 14220 Prague 4, Czech Republic

Introduction

The extracellular space (ECS) is the microenvironment of the nerve cells and an important communication channel (Nicholson, 1979; Syková, 1983; Syková, 1992; Syková, 1997; Nicholson and Syková, 1998). It includes ions, transmitters, metabolites, peptides, neurohormones, other neuroactive substances and molecules of the extracellular matrix, and directly or indirectly affects neuronal and glial cell functions. Neurons and glia release a number of neuroactive substances into the ECS, which diffuse via the ECS to their targets located on nerve as well as glial cells, frequently distant from the release sites. Transmitters which escape from synapses or are released non-synaptically diffuse through the ECS and bind to extrasynaptic, usually high-affinity, binding sites located on neurons, axons and glial cells. This type of extrasynaptic transmission is also called 'diffusion transmission' (neuroactive substances diffuse through the ECS) or 'volume transmission' (neuroactive substances move through the volume of the ECS) (Fuxe and Agnati, 1991; Bach-y-Rita, 1993; Agnati et al., 1995; Syková, 1997; Nicholson and Syková, 1998; Zoli et al., 1999). Populations of neurons can interact both by synapses and by the diffusion of ions and neurotransmitters in the ECS. Since glial cells do not have synapses, their communication with neurons is only mediated by the diffusion of ions and neuroactive substances in the ECS. This mode of communication without synapses provides a mechanism of long-range information processing in functions such as vigilance, sleep, chronic pain, hunger, depression, LTP, LTD, memory formation and other plastic changes in the CNS (Syková, 1997). The size and irregular geometry of diffusion channels in the ECS (tissue tortuosity and anisotropy) substantially affect and/or direct the movement of various neuroactive substances in the CNS (Fig. 1) and thereby

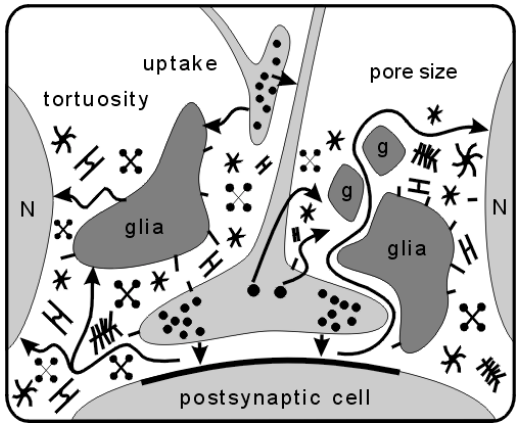

Fig. 1. Schematic of CNS architecture. The CNS architecture is composed of neurons (N), glial cells (glia), neuronal and glial processes (g), molecules of the extracellular matrix and intercellular channels between the cells. This architecture slows down the movement (diffusion) of substances in the brain, which is critically dependent on the ECS diffusion parameters volume fraction (α), tortuosity (λ) and nonspecific uptake (k').

*Corresponding author. Tel.: (+420 2) 475 2204; Fax: (+420 2) 475 2783; e-mail: sykova@biomed.cas.cz

modulate neuronal signalling, neuron-glia communication and volume transmission.

Any change in the ECS diffusion parameters could result in the impairment of signal transmission and contribute to functional deficits and to neuronal damage. Dynamic changes in ECS ionic composition, volume and geometry accompany neuronal activity, neuronal loss, glial development and proliferation, aging, CNS injury, anoxia/ischemia, spreading depression, tumors, inflammmation, dyemyelination and many other brain pathological states.

Extracellular space composition

Cellular elements and blood vessels fill about 80% of the total CNS tissue volume and the remaining portion (15–25%) is the extracellular space. ECS ionic changes resulting from transmembrane ionic shifts during neuronal activity depolarize neighboring neurons and glial cells, enhance or depress their excitability, and affect ion channel permeability (Syková, 1983; Walz, 1989; Chesler, 1990; Syková, 1992; Deitmer and Rose, 1996; Syková, 1997). These ionic changes may also lead to the synchronization of neuronal activity and stimulate glial cell function.

In the mammalian CNS, the average ionic constituents of the ECS are basically the same as in the cerebrospinal fluid (mEq/kg H_2O): about 148 Na^+, 130 Cl^-, 3 K^+, 22 HCO_3^-, 2.5 Ca^{2+}, 1.7 Mg^{2+}, 5.3 glucose, 0.9 amino acids, 6.5 urea, osmolality 305, pH 7.27 (rabbit CSF, Dawson and Segal, 1996). However, in vivo measurements with ion-selective microelectrodes have revealed local changes in ECS ionic composition resulting from neuronal activity. The local changes in ion activity are localized to areas of high spontaneous activity (Syková et al., 1974; Syková et al., 1983), in areas being activated by electrical or adequate stimuli, e.g. tactile, visual, auditory, taste aversive and painful stimuli (Singer and Lux, 1975; Svoboda et al., 1988; Johnston et al., 1989; Syková et al., 1990; Syková and Svoboda, 1990), and during pathological states like anoxia, seizures, injury, spreading depression etc. Ionic and volume homeostasis in the CNS is maintained by a variety of mechanisms present in neurons as well as in glial cells. It was shown in a number of studies in vivo as well as *in vitro* that changes in extracellular K^+ concentration ($[K^+]_e$), alkaline and acid shifts in pH_e and a decrease in extracellular Ca^{2+} concentration ($[Ca^{2+}]_e$) accompany neuronal activity in different brain regions (for review see Syková, 1983; Chesler, 1990; Syková, 1992).

Other important chemical components of the ECS are substances involved in metabolism, particularly glucose and dissolved gases (O_2 and CO_2). The presence of HCO_3^- and CO_2 forms a powerful buffering system which controls extracellular and intracellular pH. The ECS also contains free radical scavengers such as ascorbate and glutathione (Rice, 2000), which may counteract some potentially lethal products of oxygen metabolism. In addition, the ECS contains amino acids like glutamate and aspartate, catecholamines, indolamines such as dopamine and serotonin, various opioid peptides, NO and growth hormones. Transmitters in the ECS bind to extrasynaptically located high affinity binding sites on neurons and glia.

The solution in the ECS is, however, not a simple salt solution. It has become apparent that long chain polyelectrolytes, either attached or unattached to cellular membranes, are present in the ECS. The ECS also contains a number of glycosaminoglycans (e.g. hyaluronate), glycoproteins and proteoglycans that constitute the extracellular matrix (ECM). It has been shown that the molecular content of the ECM, e.g. chondroitin sulphate proteoglycan, fibronectin, tenascin, laminin, etc. (Thomas and Steindler, 1995; Celio et al., 1998), dynamically changes during development, aging, wound healing and many pathological processes. ECM molecules are produced by both neurons and glia. These molecules have been suggested to cordon off distinct functional units in the CNS (groups of neurons, axon tracts, and nuclear groups). As shown in Fig. 1, these large molecules can slow down the movement (diffusion) of various neuroactive substances through the ECS. More importantly, these molecules may hinder diffusion of molecules so that they are confined to certain places, while diffusion to other brain regions will be facilitated.

Cells, particularly glia, maintain not only ECS ionic homeostasis but also ECS volume homeostasis (by swelling and shrinking during ionic

shifts). They produce various extracellular matrix molecules (Celio et al., 1998) and therefore produce diffusion barriers. Glial cells when hypertrophied or proliferating form diffusion barriers (Syková, 1997; Roitbak and Syková, 1999) and in this way critically affect the permissiveness of the tissue, synaptic as well as volume transmission, activity-dependent synaptic plasticity, neurogenesis and regeneration.

Diffusion parameters of the ECS

The diffusion of substances in a free medium, such as water or diluted agar, is described by Fick's laws. In contrast to a free medium, diffusion in the ECS of the nervous tissue is hindered by the size of the extracellular clefts, the presence of membranes, fine neuronal and glial processes, macromolecules of the extracellular matrix and charged molecules, and also by cellular uptake (Fig. 1). To take these factors into account, it was necessary to modify Fick's original diffusion equations (Nicholson and Phillips, 1981; Nicholson and Syková, 1998; Nicholson et al., this volume). First, diffusion in the CNS is constrained by the restricted volume of the tissue available for the diffusing particles, i.e. by the extracellular space volume fraction (α), which is a dimensionless quantity and is defined as the ratio between the volume of the ECS and the total volume of the tissue ($\alpha = V_{ECS}/V_{TOT}$). It is now evident that the ECS in adult brain amounts to about 20% of the total brain volume, i.e. $\alpha = 0.2$ (Fig. 2, Table 1). Second, the free diffusion

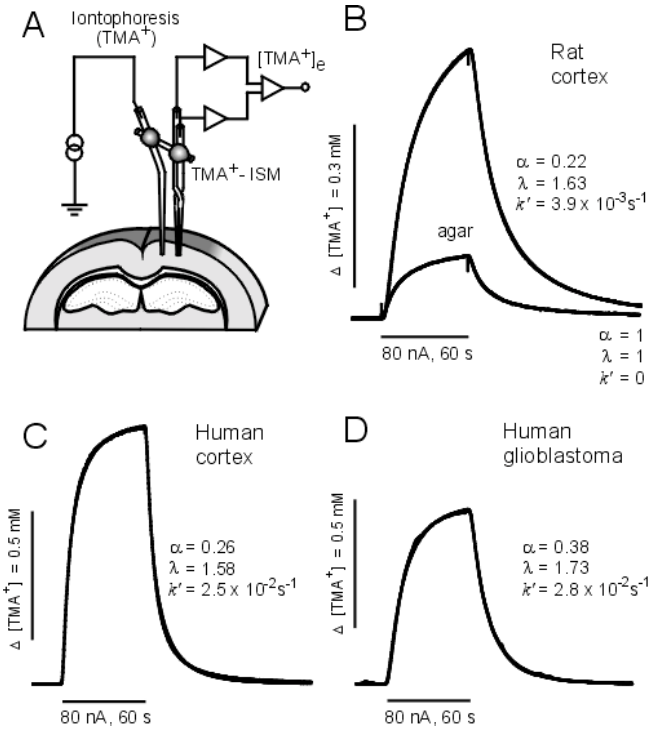

Fig. 2. A: Schema of the experimental arrangement. TMA^+-selective double-barrelled ion-selective microelectrode (ISM) was glued to a bent iontophoresis microelectrode. The separation between electrode tips was 80–200 μm. B: TMA^+ diffusion curves in the rat somatosensory cortex in vivo and free diffusion measured with the same microelectrode array in agar. C: Typical diffusion curve recorded in a slice (submerged slices, 400 μm thick) from the human temporobasal cortex of an 18-year-old woman with pharmacoresistant epilepsy. D: Typical diffusion curve in a slice (400 μm) from a human glioblastoma (grade 4, WHO clasification). For each curve, the ECS diffusion parameters α (volume fraction) and λ (tortuosity) were extracted by appropriate nonlinear curve fitting. Experimental and theoretical curves are superimposed in each case. For each figure the concentration scale is linear.

coefficient (D) in the brain is reduced by the square of the tortuosity (λ). ECS tortuosity is defined as $\lambda = (D/ADC)^{0.5}$, where D is a free diffusion coefficient and ADC is the apparent diffusion coefficient in the brain. As a result of tortuosity (in adult brain λ amounts to 1.55–1.65, Fig. 2), D is reduced to an apparent diffusion coefficient $ADC = D/\lambda^2$. Thus, any substance diffusing in the ECS is hindered by many obstructions. Third, substances released into the ECS are transported across membranes by non-specific concentration-dependent uptake (k'). In many cases, however, these substances are transported by energy-dependent uptake systems that obey nonlinear kinetics (Nicholson, 1995). When these three factors (α, λ and k') are incorporated into Fick's law, diffusion in the CNS is described fairly satisfactorily (Nicholson and Phillips, 1981).

The real-time iontophoretic method is used to determine ECS diffusion parameters and their dynamic changes in nervous tissue in vitro as well as in vivo (Syková, 1997; Nicholson and Syková, 1998). In principle, ion-sensitive microelectrodes (ISM) are used to measure the diffusion of ions to which the cell membranes are relatively impermeable, e.g. TEA^+, TMA^+ or choline. These substances are injected into the nervous tissue by pressure or by iontophoresis from an electrode aligned parallel to a double-barreled ISM at a fixed distance (Fig. 2). Such an electrode array is made by gluing together a pressure or iontophoretic pipette and a TMA^+-sensitive ISM with a tip separation of 60–200 μm. In the case of iontophoretic application, the TMA^+ is released into the ECS by applying a current step of +80–100 nA with a duration of 40–80 sec. The released TMA^+ is recorded with the TMA^+–ISM as a diffusion curve (Fig. 2), which is then transferred to a computer. Values of the ECS volume, ADCs, tortuosity and

TABLE 1

Values of volume fraction (α) and tortuosity (λ) obtained with the real-time iontophoretic TMA^+ method in the CNS

Region	Preparation	α	λ (λ_x, λ_y, λ_z)	References
Spinal cord, dorsal horn (rat)	In vivo	0.20–0.21	1.55–1.62	(Syková et al., 1994)
dorsal horn (frog)	In vitro	0.19	1.59	(Prokopová & Syková, in press)
dorsal horn (mouse)	In vitro	0.20	1.82	(Prokopová & Syková, in press)
intermediate region (rat)	In vivo	0.22	1.54	(Šimonová et al., 1996)
ventral horn (rat)	In vivo	0.23	1.46	(Šimonová et al., 1996)
white matter (rat)	In vivo	0.18	1.56[a]	(Šimonová et al., 1996)
filum terminale (frog)	In vitro	0.32	1.42	(Prokopová & Syková, in press)
Neocortex (rat)	In vitro	0.18	1.62	(Pérez-Pinzón et al., 1995)
Neocortex (human)	In vitro	0.21–0.26	1.44–1.58	(Vargová & Syková, unpublished)
Sensorimotor cortex (rat), layer II	In vivo	0.19	1.51	(Lehmenkühler et al., 1993)
layer III	In vivo	0.20	1.63	(Lehmenkühler et al., 1993)
layer IV	In vivo	0.21	1.59	(Lehmenkühler et al., 1993)
layer V	In vivo	0.22	1.62	(Lehmenkühler et al., 1993)
layer VI	In vivo	0.23	1.65	(Lehmenkühler et al., 1993)
Sensorimotor cortex (mice)	In vivo	0.23	1.78	(Mazel & Syková, 1999)
Auditory cortex (rat)	In vivo	0.21	1.52; 1.70; 1.81	(Syková et al., 1999a)
Corpus callosum (rat)	In vivo	0.21	1.47; 1.67; 1.69	(Mazel et al., 1998)
Neostriatum (rat)	In vitro	0.21	1.54	(Rice & Nicholson, 1991)
Hippocampus (rat) CA1 st. pyramidale	In vivo	0.21	1.39; 1.65; 1.80	(Mazel et al., 1998)
CA1 st. radiatum	In vivo	0.22	1.52; 1.61; 1.82	(Mazel et al., 1998)
Dentate gyrus	In vivo	0.22	1.49; 1.59; 1.68	(Mazel et al., 1998)
CA3 st. pyramidale	In vivo	0.22	1.50; 1.62; 1.69	(Mazel et al., 1998)
CA3 st. radiatum	In vivo	0.20	1.53; 1.58; 1.70	(Mazel et al., 1998)
Hippocampus (mice) CA1	In vivo	0.20	1.69[a]	(Mazel & Syková, 1999)
Cerebellum, molecular layer (rat)	In vivo	0.21	1.55[a,b]	(Nicholson & Phillips, 1981)
Cerebellum, molecular layer (turtle)	In vitro	0.31	1.44, 1.95, 1.58	(Rice et al., 1993)
Cerebellum, granular layer (turtle)	In vitro	0.21	1.77	(Rice et al., 1993)

[a] = measurements did not take anisotropy into account
[b] = measurements did not take non-specific TMA_4/TEA^+ uptake into account

non-specific cellular uptake are extracted by a nonlinear curve-fitting simplex algorithm applied to the diffusion curves (see Nicholson et al., this volume).

The other methods that are also used to study ECS volume and geometry, e.g. intrinsic optical signals (IOS), tissue resistance, integrative optical imaging (IOI) and nuclear magnetic resonance (NMR), are less comprehensive because they can measure only relative changes in the ECS diffusion parameters or only some of the three diffusion parameters (Van Harreveld et al., 1971; Matsuoka and Hossmann, 1982; Korf et al., 1988; Nicholson and Tao, 1993; Andrew and MacVicar, 1994). Integrative optical imaging is used to measure the *ADC*s of molecules tagged with fluorescent dye, while recordings of intrinsic optical signals, either light transmittance or light reflectance, are believed to reflect changes in the ECS volume; however, direct evidence is missing. On the other hand, diffusion-weighted NMR methods provide information only about the water diffusion coefficient (Benveniste et al., 1992; Latour et al., 1994; Norris et al., 1994; Van der Toorn et al., 1996). Although the correlation between water diffusion maps and changes in cell volume and ECS diffusion parameters can be very good, it is still not well understood (see below).

Using a light transmittance method (IOS, intrinsic optical signals), we recently found that changes in the ECS volume in brain slices measured by the TMA method have a different time course than those revealed by IOS. Simultaneous measurements using IOS and the TMA method were used to determine the absolute values of the ECS volume fraction α, tortuosity λ and non-specific uptake k' in the dorsal horns of rat spinal cord slices (Vargová et al., 1999). Cell swelling was evoked by a 45 min exposure to hypotonic solutions, elevated potassium or glutamate receptor agonists. Hypotonic solution (160 mOsmol/kg), 50 or 80 mM K^+, or NMDA (10^{-4}) induced a decrease in α of 45–85%, which peaked at 10–15 min, while an increase in IOS of 20–35% peaked in the first five minutes. After the initial peak, IOS quickly decreased to control levels, while the changes in α and λ persisted throughout the application of the test solutions (Fig. 3). There was also no correlation with the changes in ECS tortuosity and uptake. These data show that there is no simple correlation between ECS volume and IOS changes.

Neuroactive substances released constantly into the ECS will accumulate in this limited volume more rapidly than in free solution. Tortuosity (which is absent in a free medium) also causes a greater and more rapid accumulation of released substances. CNS tortuosity reduces the diffusion coefficient for small molecules by a factor of about 2.5 in many CNS regions. Larger molecules (with a relative molecular mass above 10 kDa), have a smaller diffusion coefficient than small molecules and are significantly more hindered in their diffusion, and therefore exhibit larger tortuosity (Nicholson and Tao, 1993; Tao et al., 1995; Tao and Nicholson, 1996). However, even large proteins, e.g. negatively charged globular proteins such as bovine serum albumin (66 kDa), or dextrans of 70 kDa, still migrate through the narrow interstices of brain slices (Nicholson and Tao, 1993; Tao and Nicholson, 1996). Recently, the diffusion properties of two types of rather large copolymers of N-(2-hydroxypropyl)methacrylamide (HPMA), developed as water-soluble anti-cancer drug carriers, were studied in rat cortical slices – HPMA polymeric chains with $M_r = 1{,}000{,}000$ and star-like systems, containing either albumin (179,000 M_r) or immunoglobulin (IgG) (319,000 M_r) in the center with HPMA side branches. Using the integrative optical imaging method and pressure microinjection of fluorescein-tagged polymers, the apparent diffusion coefficients (*ADC*) were obtained in rat cortical slices (Vargová et al., 1998). Surprisingly, long-chain HPMA polymers diffuse through the ECS with the same tortuosity as small molecules such as TMA. However, when the HPMA is configured into a more bulky globular molecule, the tortuosity increases to about 2.3. The tortuosity for long-chain HPMA is always found to be smaller than the tortuosity for globular copolymers (Prokopová et al., 1999). These data show that rather than M_r, the shape of the substance is the limiting factor in its movement through the extracellular space.

Diffusion inhomogeneity and anisotropy

ECS diffusion parameters are different in different parts of the CNS (Table 1). For example, it has been

recognized that the TMA^+ diffusion parameters in the sensorimotor cortex of adult rat in vivo are heterogeneous (Lehmenkühler et al., 1993). The mean volume fraction gradually increases from $\alpha = 0.19$ in cortical layer II to $\alpha = 0.23$ in cortical layer VI. These typical differences are apparent in each individual animal. In subcortical white matter (corpus callosum) the volume fraction is always lower than in cortical layer VI, often between 0.19–0.20 (Voříšek and Syková, 1997a; Mazel et al., 1998). There is also a heterogeneity in the spinal cord, the mean values of the volume fraction being highest in the ventral horn and lowest in the white matter (Syková et al., 1994; Šimonová et al., 1996; Prokopová et al., 1997). Similar α values ($\alpha = 0.21$–0.22) have been found throughout the rat brain. In slices from human cortex (temporal and frontal lobe), recently obtained α values were not much different – they ranged between 0.21–0.26 (Fig. 2). Also the α values in other species such as mice, frog and turtle have been in the same range, with the exception of slices from frog filum

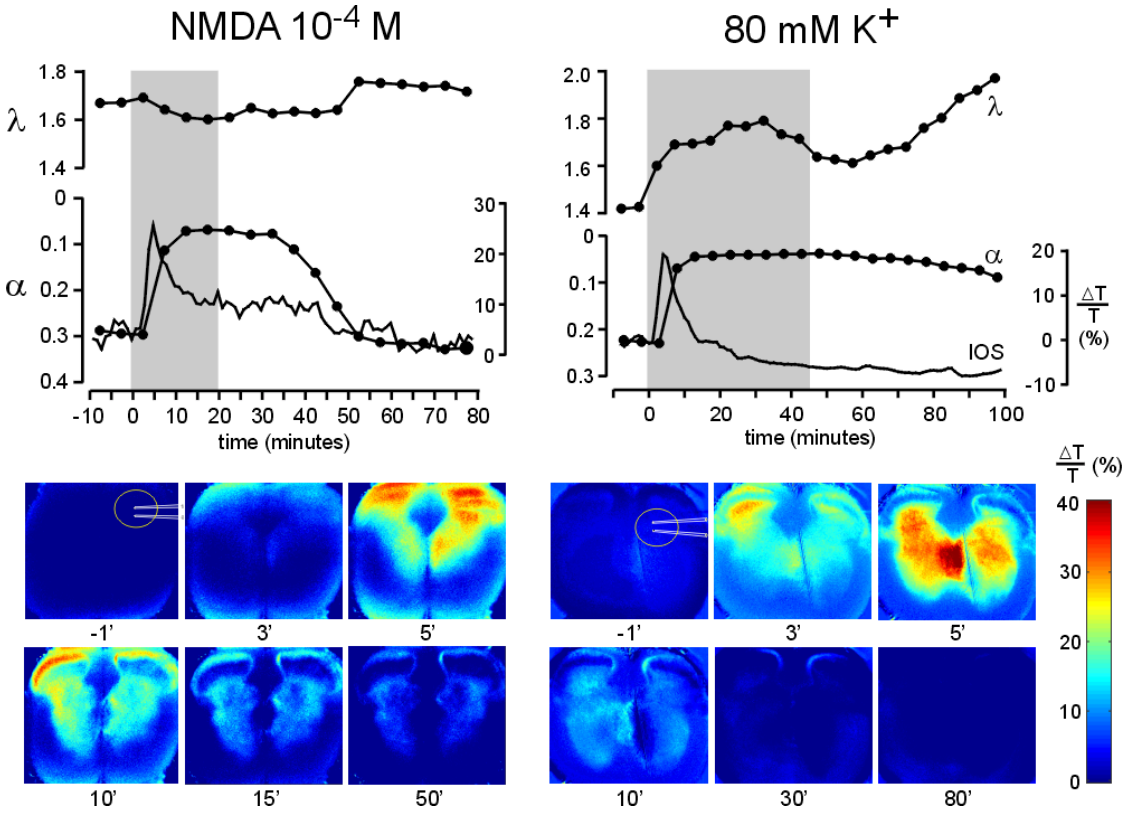

Fig. 3. Simultaneous measurements of the TMA^+ diffusion parameters and intrinsic optical signal (IOS) in spinal cord slices (400 µm thick) of a 14-day-old rat. Changes in TMA diffusion parameters α (ECS volume fraction) and λ (ECS tortuosity) before, during and after perfusion of the slice with NMDA (10^{-4}) or 80 mM K^+ were extracted by appropriate nonlinear diffusion curve fitting and plotted with the same time course as the IOS. Below: IOS images taken 1 minute before application (–1'; control) and 3', 5', 10', 15', 30', 50' and 80' minutes after application of NMDA or K^+. Cellular, particularly glial, swelling results in an ECS volume decrease and, only in the case of K^+ application, also in a tortuosity increase. While the changes in TMA diffusion parameters persist for the whole application period and long after, the changes in IOS decrease with time. It is also evident that the time course of the IOS signal peaks faster than the changes in ECS volume and tortuosity. There is, therefore, no simple correlation between the IOS signal and ECS volume changes.

terminale ($\alpha = 0.32$) and turtle cerebellar molecular layer ($\alpha = 0.31$) (Table 1).

By introducing the tortuosity factor into diffusion measurements in the CNS, it soon becomes evident that diffusion is not uniform in all directions and that it is affected by diffusion barriers. This so-called anisotropic diffusion preferentially channels the movement of neuroactive substances in the ECS in one direction (e.g. along axons) and may, therefore, be responsible for a certain degree of specificity in volume transmission. Significant differences in tortuosity have been found in various brain regions, showing that the local architecture is different. There is increasing evidence that diffusion in brain tissue is anisotropic; isotropy is defined as the state of constant λ in any direction from a point source, while anisotropy indicates a difference in λ along different axes. To test for anisotropy, the ECS diffusion parameters are measured in three orthogonal axes x, y and z. Indeed, anisotropic diffusion was described using the TMA^+-method in the white matter of the corpus callosum (Fig. 4) and spinal cord (Prokopová et al., 1997; Voříšek and Syková, 1997a) as well as in the gray matter of the molecular layer of the cerebellum (Rice et al., 1993), in the hippocampus (Figs. 4 and 5) (Mazel et al., 1998) and in the auditory (Fig. 4) but not in the somatosensory cortex (Syková et al., 1999a). Using MRI, evidence of anisotropic diffusion in white matter was found in cat brain (Moseley et al., 1990) as well as in human brain (Le Bihan et al., 1993). Therefore, not only the diffusion of molecules such as TMA^+ or dextrans, but even the diffusion of water, is modified by various cellular structures including myelin sheaths. Because of the distinct diffusion characteristics, the extracellular molecular traffic will be different in various brain regions. The anisotropy and inhomogeneity of white and gray matter could enable different modes of diffusion transmission in these regions.

Recently we also obtained evidence that changes in anisotropy during development, aging and pathological states, mediated by the different structure of neurons, dendrites, axons, glial processes, myelin sheaths and extracellular matrix, can affect the migration of substances in the ECS (e.g preferred diffusion in one direction is lost) and may, therefore, account for an impairment of volume transmission (see below).

Diffusion parameters and neuronal activity

Transmembrane ionic fluxes during neuronal activity are accompanied by the movement of water and cellular, presumably particularly glial (see below), swelling. Changes in ECS diffusion parameters (ECS volume decrease, tortuosity increase and *ADC* decrease) are the consequence of activity-related transmembrane ionic shifts and cellular swelling. In the spinal cord of the rat or frog, repetitive electrical stimulation results in an ECS volume decrease from about 0.24 to 0.12–0.17, i.e. the ECS volume decreases by as much as 30–50% (Syková, 1987; Svoboda and Syková, 1991). The ECS volume in the spinal dorsal horn of the rat also decreases by 20–50% after injury of the ipsilateral hind paw evoked by subcutaneous injection of turpentine or after thermal injury. The changes in ECS diffusion parameters persist for many minutes (30 min after electrical stimulation or even 120 min after peripheral injury) after stimulation has ceased, suggesting long-term changes in neuronal excitability, neuron-glia communication and volume transmission.

Role of glia in ECS volume and geometry changes

It was shown in a number of studies that astrocyte swelling is an early event in numerous pathological states, accompanied by an elevation of $[K^+]_e$ (Kimelberg and Ransom, 1986; Kimelberg, 1991; Kimelberg et al., 1992). It was also shown that in the isolated turtle cerebellum exposed to hypotonic medium, volume fraction decreased to 0.12, while in hypertonic medium it increased to as much as 0.60 (Križaj et al., 1996).Cell swelling and astrogliosis (manifested as an increase in GFAP) were also evoked in isolated rat spinal cords of 4–21-day-old rats by incubation in either 50 mM K^+ or hypotonic solution (235 mOsmol/kg). Application of K^+ or hypotonic solution resulted at first in a decrease in the ECS volume fraction and in an increase in tortuosity in spinal gray matter (Fig. 6). These changes resulted from cell swelling, since the total water content (TW) in the spinal cord was

unchanged and the changes were blocked in Cl-free solution and slowed down by furosemide and bumetanide (Syková et al., 1999c). During a continuous 45 min application of 50 mM K^+, α and λ often start to return towards control values, apparently due to the shrinkage of previously swollen cells since TW remains unchanged. This return is blocked by the gliotoxin fluoroacetate, suggesting that most of the changes are due to the swelling of glia. A 45 min application of 50 mM K^+ and, to a lesser degree, of hypotonic solution evokes astrogliosis, which persists after washing out these solutions with physiological saline. During astrogliosis λ increases again to values as high as 2.0, while α either returns to or increases above control values (Syková et al., 1999c). This

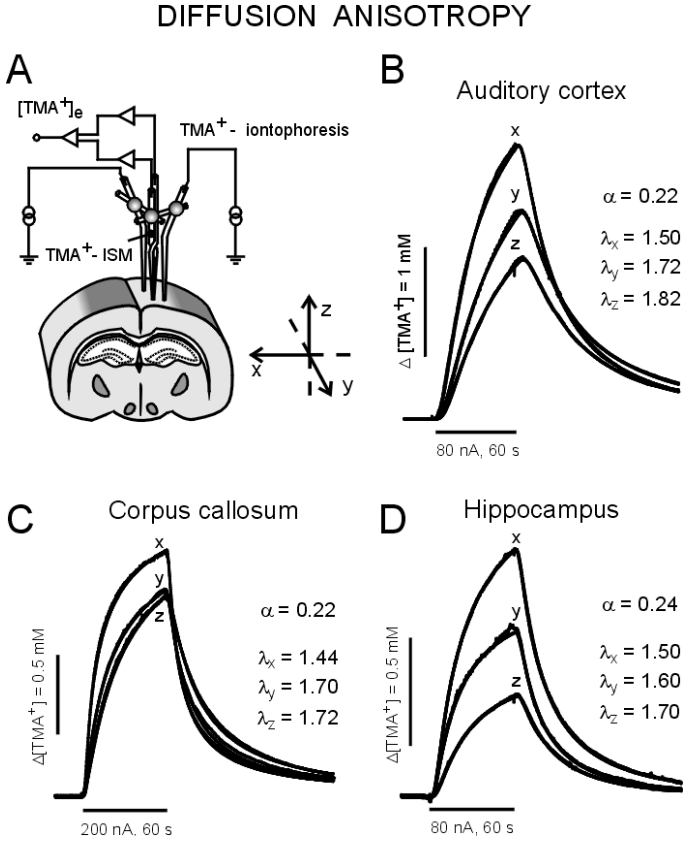

Fig. 4. Anisotropic diffusion in the rat brain. A: Schema of experimental arrangement to study diffusion anisotropy. A TMA^+-selective double-barrelled ion-selective microelectrode (ISM) was glued to two bent iontophoresis microelectrodes. The tips of the 3 pipettes formed a 90° horizontal angle for simultaneous measurements along the *x*- and *y*-axes. Similarly, for measurements along the *z*-axis, one iontophoresis pipette tip was lowered 110–180 μm below the tip of the ISM. B: Anisotropic diffusion in the auditory cortex. C: In the corpus callosum diffusion in the direction perpendicular to the orientation of the axons (*y*- and *z*- axes) is compromised by the number of myelin sheaths. D: Anisotropic diffusion in the dentate gyrus of the hippocampus. B, C, D: TMA^+ diffusion curves (concentration-time profiles) were measured along three orthogonal axes (*x* – mediolateral, *y*- rostrocaudal, *z* – dorsoventral). The slower rise in the *z* than in the *y* direction and in the *y* than in the *x* direction indicates a higher tortuosity and more restricted diffusion. The amplitude of the curves show that TMA^+ concentration, at approximately the same distance from the tip of the iontophoresis electrode, is much higher along the *x*-axis than along the *y*-axis and even higher than along the *z*- axis (λ_x, λ_y, λ_z).This can be explained if we realize that TMA^+ concentration decreases with the 'diffusion distance' from the iontophoretic micropipette and that the real 'diffusion distance' is not *r* but λr. Note that the actual ECS volume fraction α is 0.22–0.24 and can be calculated only when measurements are done along the *x*-, *y*- and *z*-axes.

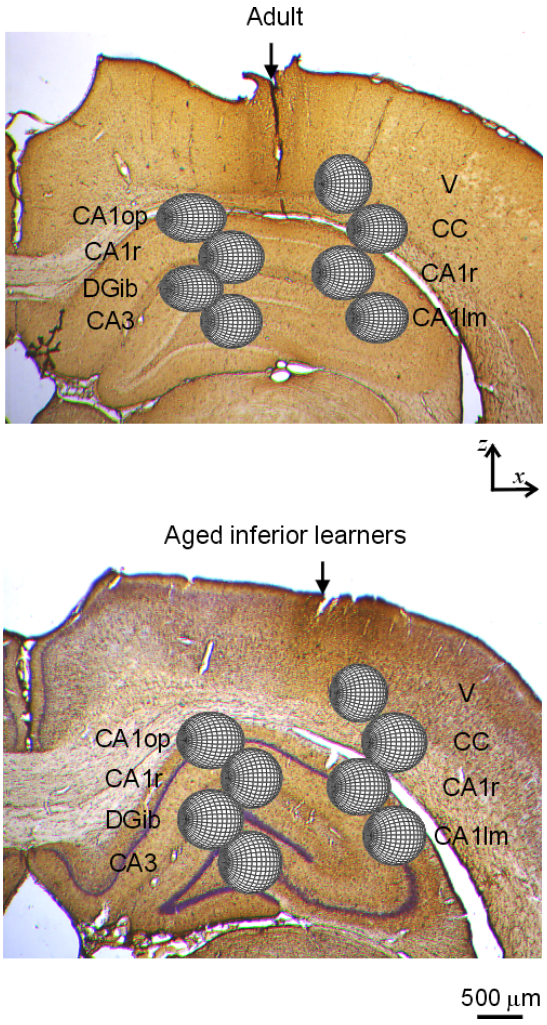

Fig. 5. Diffusion parameters in a young adult (3 months old) and aged (28 months old) rat with a learning deficit in the Morris water maze. Data were recorded in anesthetized animals; microelectrode tracks were verified after the experiments (see arrows). Iso-concentration surfaces for a 1 mM TMA^+ concentration contour 60 seconds after the onset of a 80 nA iontophoretic pulse. The surfaces were generated using the actual values of volume fraction and tortuosity. The ellipsoid represents anisotropic diffusion in a young adult rat. The larger sphere in an aged rat corresponds to isotropic diffusion and to a lower ECS volume fraction. It demonstrates that diffusion from any given source will lead to a higher concentration of substances in the surrounding tissue and a larger action radius in aged rats than in young adults. Anisotropy is almost lost in the aged rat.

persistant increase in λ after washout is also found in white matter. These data show that glial swelling and astrogliosis are associated with a persistant increase in ECS diffusion barriers.

Astrogliosis. Many pathological processes in the central nervous system are accompanied by a loss of cells or neuronal processes, astrogliosis, demyelination, and changes in the extracellular matrix, all of which may affect the apparent diffusion coefficients of neuroactive substances. Several animal models have been developed to study changes in ECS diffusion parameters. Brain injury of any kind elicits reactive gliosis, involving both hyperplasia and hypertrophy of astrocytes, which show intense staining for glial fibrillary acidic protein (GFAP) (Norton et al., 1992). Astrogliosis is also a typical characteristic of cortical stab wounds in rodents (Norton et al., 1992). The lesion is typically accompanied by an ECS volume increase and a substantial tortuosity increase to mean values of α of about 0.26 and λ of about 1.77 (see below) (Roitbak and Syková, 1999).

Similarly, both the size of the ECS (α) and, surprisingly, also λ are significantly higher in cortical grafts than in host cortex, about 0.35 and 1.79, respectively, as is also the case in gliotic cortex after stab wounds. Both α and λ are increased in cortical grafts of fetal tissue transplanted to the midbrain, where severe astrogliosis compared to host cortex is found, but not in fetal grafts placed into a cavity in the cortex, where only mild astrogliosis occurs (Syková et al., 1999b). Another characteristic feature of cortical grafts into midbrain is the variability of α and λ; the different values found at various depths of the grafts correlate with the morphological heterogeneity of the graft neuropil. These measurements show that even when the ECS in gliotic tissue or in cortical grafts is larger than in normal cortex, the tortuosity is still higher, and the diffusion of chemical signals in such tissue may be hindered. Limited diffusion may also have a negative impact on the viability of grafts in host brains. Compared to host cortex, immunohistochemistry shows myelinated patches and a larger number of hypertrophic astrocytes in areas of high λ values, suggesting that more

numerous and/or thicker glial cell processes might be a cause of the increased tortuosity.

Diffusion properties in CNS of GFAP+/+ and GFAP–/– mice. To assess the function of glial fibrillary acidic protein (GFAP), the main component of astroglial intermediate filaments, we studied astrocyte membrane properties and the regulation of extracellular space volume in GFAP-negative mice (GFAP–/–). The GFAP gene was disrupted via targeted mutation in embryonic stem cells (Pekny et al., 1995). We compared the ECS diffusion parameters in isolated spinal cord (gray matter) of GFAP–/– and +/+ mice at postnatal days 5, 8 (P5, P8) and in the adult brain (P50–80). We found no difference in ECS diffusion parameters in GFAP–/– vs. +/+ mice at any age or in any brain region. In both groups, λ gradually increases with age to 1.7–1.8 and α decreases to about 0.2 at P50–80 (Table 2). However, during the application of 50 mM K^+ a significantly greater decrease in volume fraction and increase in tortuosity is seen in GFAP +/+ than in –/– mice (Fig. 6).

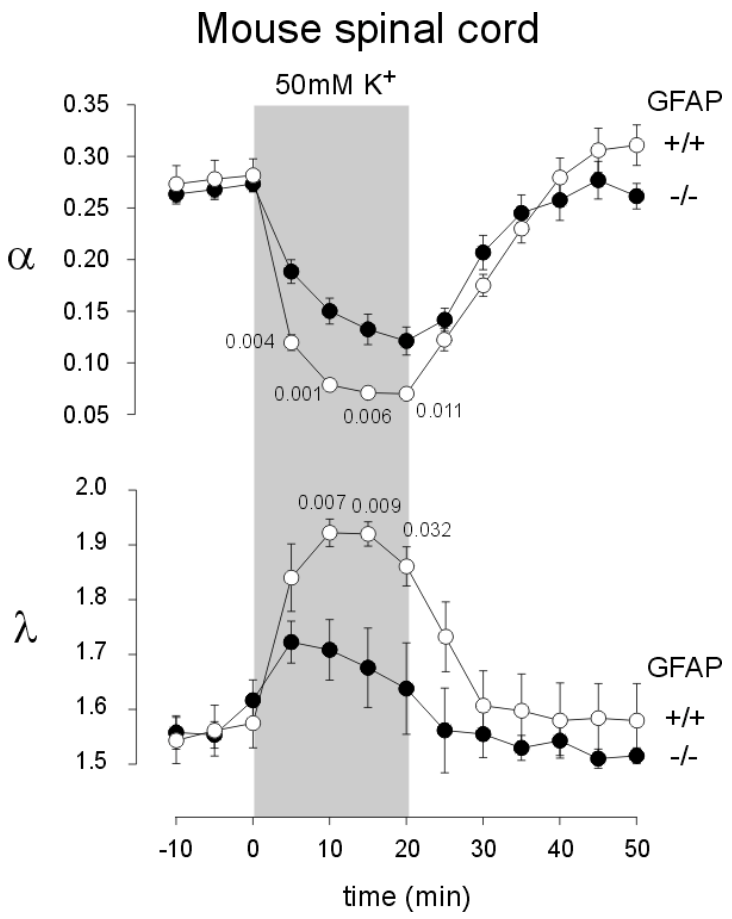

Fig. 6. The effect of 50 mM K^+ on ECS diffusion parameters in the gray matter of mouse spinal cord as measured in GFAP +/+ and GFAP –/– mice (mean ± S.E.M., $n = 4$ in each). Each data point represents calculated α and λ values recorded at 5-minute intervals. Note that the time course of ECS volume decrease evoked by cell swelling is slower and smaller in GFAP –/– mice; as well, the tortuosity increase is significantly smaller (p values are shown where the difference is significant).

We have also found that a wave of spreading depression elicited in the cortex of GFAP +/+ mice by a needle prick is faster than that in GFAP –/– mice, although the final maximal values of the ECS volume fraction decrease and tortuosity increase are not significantly different (Mazel and Syková, unpublished results).

Using the whole-cell patch-clamp technique, we compared the reversal potential (V_{rev}) of astrocytes and their responses to elevated K^+ and glutamate. Depolarization of GFAP–/– astrocytes in spinal cord slices by 50 mM K^+ is significantly slower than that of GFAP +/+ ones. Although the maximal amplitude of the response is not significantly different, its peak is reached later in GFAP –/– astrocytes compared to GFAP +/+ astrocytes. The inward currents evoked by 1 mM glutamate in GFAP–/– astrocytes are smaller and slower than in GFAP+/+ ones by about 40%. In other words, the GFAP–/– astrocytes respond more slowly to high K^+ and with smaller inward currents to glutamate (Anděrová et al., 1999).

Our results show that astrocytes in GFAP+/+ and GFAP–/– mice may have different membrane properties, particularly under pathological conditions, e.g. anoxia, ischemia, seizures or repetitive

TABLE 2

Mean values of the ECS diffusion parameters during development, aging and pathological states as measured by the TMA^+-method. All data from rats in vivo

Status	Region	α	λ (λ_x, λ_y, λ_z)	References
Development (rat)	Cortex (P2)	0.36–0.4	1.59–1.68	(Lehmenkühler et al., 1993)
	Corpus callosum (P2)	0.46	1.58	(Lehmenkühler et al., 1993)
	Spinal cord, dorsal horn (P5)*	0.25	1.52	(Prokopová et al., 1997)
	Spinal cord, white matter (P8)*	0.27	1.33; 1.52	(Prokopová et al., 1997)
Aging (rat)	Cortex	0.19	1.57	(Syková et al., 1998b)
	Corpus callosum	0.19	1.48; 1.69; 1.71	(Syková et al., 1998b)
	Hippocampus CA1	0.19	1.49; 1.59; 1.72	(Syková et al., 1998b)
	Dentate gyrus	0.19	1.51; 1.54; 1.69	(Syková et al., 1998b)
	Hippocampus CA3	0.18	1.52; 1.52; 1.66	(Syková et al., 1998b)
Chronic pain (rat)	Spinal cord	0.12	—	(Jendelová & Syková, 1991)
GFAP –/– (mice)	Sensorimotor cortex	0.23	1.69	(Mazel & Syková, 1999)
	Corpus callosum	0.24	1.60 (λ_y)	(Mazel & Syková, 1999)
	Hippocampus CA1	0.25	1.61 (λ_y)	(Mazel & Syková, 1999)
	Spinal cord, dorsal horn*	0.22	1.84	(Prokopová et al., 1998)
SD (rat)	Cortex	0.09	2.01	(Richter et al., 1999)
SD GFAP +/+ (mice)	Cortex	0.05	2.38	(Mazel & Syková, unpublished)
SD GFAP –/– (mice)	Cortex	0.07	1.76	(Mazel & Syková, unpublished)
Hypoxia (rat)	Spinal cord	0.16	1.62	(Syková et al., 1994)
Terminal anoxia (rat)	Spinal cord	0.07	2.2	(Syková et al., 1994)
	Cortex	0.07	1.63[b]	(Lundbaek & Hansen, 1992)
	Cortex	0.06	2.00	(Voříšek & Syková, 1997b)
	Corpus callosum	0.05	2.10[a]	(Voříšek & Syková, 1997b)
Recovery after anoxia (rat)	Spinal cord	0.30	1.63	(Syková et al., 1994)
Hypernatremia (rat)	Cortex	0.10–0.15	1.65	(Cserr et al., 1991)
Astrogliosis-stab wounds (rat)	Cortex	0.30	1.93	(Roitbak & Syková, 1999)
X-irradiation acute state (rat)	Cortex	0.48–0.51	1.42–1.06	(Syková et al., 1996
X-irradiation chronic state (rat)	Cortex	0.34–0.55	1.56–1.81	(Syková et al., 1996)
EAE (rat)	Spinal cord, dorsal horn	0.28	1.40	(Šimonová et al., 1996)
	Spinal cord, ventral horn	0.47	1.48	(Šimonová et al., 1996)
	Spinal cord, white matter	0.30	1.48	(Šimonová et al., 1996)
Cortical grafts (rat)	Midbrain	0.34	1.78	(Syková et al., 1999b)
Tumor (human)*	Glioblastoma (gr.4–5)	0.34	1.66	(Vargová & Syková, unpublished)

* in vitro preparation

[a] = measurements did not take anisotropy into account

[b] = measurements did not take non-specific TMA^+/TEA^+ uptake into account

stimulation. GFAP as a structural protein apparently may also affect the ability of astrocytes to change their volume during swelling.

Diffusion parameters and extracellular matrix

ECM molecules and other large molecules can also affect the tortuosity of the ECS. Their possible effect on changes in TMA^+ diffusion parameters has been studied in rat cortical slices (Tao et al., 1995; Vargová et al., 1998) and in isolated rat spinal cord (Prokopová et al., 1996). Superfusion of the slice or spinal cord with a solution containing either 40-kDa or 70-kDa dextran or hyaluronic acid (HA) results in a significant increase in λ. In standard physiological solution, λ is about 1.57, while in a 1% or 2% solution of 40-kDA or 70-kDa dextran, λ increases to about 1.72–1.77. Application of a 0.1% solution of HA (1.6×10^6 Da) results in an increase in λ to about 2.0 (Fig. 7A). The α is either unchanged or it decreases by only about 10%, suggesting that these substances have no effect on cell volume and the viability of the preparation.

Modification of the extracellular matrix can also be achieved by enzymatic treatment. Chondroitin sulphate proteoglycans are essential components of the extracellular matrix, forming so-called perineuronal nets surrounding neurons in cortex and hippocampus. There is also increasing evidence that N-CAM, the protein backbone of polysialic acid (PSA), is involved in synaptic plasticity. PSA, which is almost exclusively carried by N-CAM, is a major modulator of cell adhesion and is high in areas of continuous neurogenesis, neuronal migration, neurite extension and synapse formation. It has been found that mice treated with chondroitinase ABC or with antibodies against N-CAM and transgenic mice lacking N-CAM gene have impaired LTP (Becker et al., 1996; Muller et al., 1996). It has also been demonstrated that hydrated PSA influences a sufficiently large volume at the cell surface to exert broad steric effects, and that the removal of PSA causes a detectable change in the intercellular space. By contrast, chondroitin sulphate has been found to have little influence on the intercellular space (Yang et al., 1992).

We therefore used a single intracortical injection

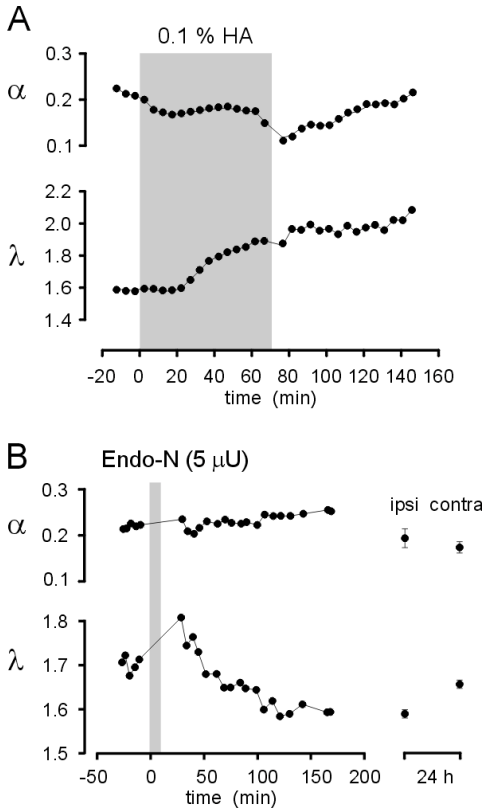

Fig. 7. Typical experiments showing the effect of hyaluronic acid and endo-neuraminidase on ECS volume fraction α and tortuosity λ. A: An isolated spinal cord was incubated in a 0.1% solution of hyaluronic acid. Note the increase in tortuosity with only about a 10% decrease in the ECS volume fraction α. B-Endo-N: Effect of endo-neuraminidase injection in the cortex of adult (3–6-month-old) rats. Two kinds of experiments were done: for acute treatment, the electrode array for TMA^+ diffusion measurement was introduced into the cortex and several control diffusion curves were taken. Clostridium neuraminidase (5 μU) dissolved in 500 nl ACSF was then applied for 10 min by pressure injection using a micropipette glued to the measuring electrode array at an inter-tip distance of 500 μm. ECS diffusion parameters were then followed for approximately 3 hours. In chronic experiments, a similar injection in anesthetized animals was made, the animals were returned to their cages, and diffusion measurements were performed 24 hours after injection. Note that immediately after neuraminidase application there was a transient decrease in ECS volume fraction accompanied by an increase in tortuosity, apparently caused by the injection. After one hour a long-lasting increase in ECS volume fraction and decrease in tortuosity occurred. These changes persisted at 24 hours after Endo-N application. No changes were found in the contralateral hemisphere.

0.5 μl) or chondroitinase ABC (10 μU) and studied the acute (3 hours) and chronic (24 hours) effects of this treatment on ECS diffusion parameters. Fig. 7B shows the effect of endo-N in rat cortex. A significant decrease in tortuosity is already found in the ipsilateral hemisphere 2 hours after injection and persists at 24 hours (Mazel and Syková, unpublished data). There is also a small but significant increase in the ECS volume fraction in the first 3 hours after injection that is not found at 24 hours. Similar changes have also been found in spinal cord slices incubated for 2 hours in endo-N or with chondroitinase (Syková and Prokopová, unpublished data).

A decrease in tortuosity and a loss of anisotropy that might be attributed to changes in the ECM have also been found during aging. This decrease correlates with the disapperance of fibronectin and chondroitin sulphate proteoglycans, forming perineuronal nets around granular and pyramidal cells in the hippocampus of young adult rats (Syková et al.,1998b). These results suggest that bigger molecules such as 40- and 70-kDa dextran, hyaluronic acid and molecules of the extracellular matrix may slow down the diffusion of small molecules such as TMA^+ (74 Da), ions, transmitters, metabolites etc. in the ECS.

ECS in pathological states

Pathological states, e.g. anoxia/ischemia, are accompanied by a lack of energy, seizure activity, the excessive release of transmitters and neuroactive substances, neuronal death, glial cell loss or proliferation, glial swelling, the production of damaging metabolites including free radicals and the loss of ionic homeostasis. Others are characterized by inflammation, edema or demyelination. It is therefore evident that they will be accompanied not only by substantial changes in ECS ionic composition (for review see Syková, 1983; Syková, 1992) but also by various changes in ECS diffusion parameters according to the different functional and anatomical changes.

Anoxia/ischemia

Dramatic K^+ and pH_e changes occur in the brain and spinal cord during anoxia and/or ischemia (Syková, 1992; Syková et al., 1994; Xie et al., 1995). Within 2 minutes after respiratory arrest in adult rats, blood pressure begins to increase and pH_e begins to decrease (by about 0.1 pH unit), while $[K^+]_e$ remains unchanged. With the subsequent blood pressure decrease, the pH_e decreases by 0.6–0.8 pH units to pH 6.4–6.6. This pH_e decrease is accompanied by a steep rise in $[K^+]_e$ to about 50–70 mM; decreases in $[Na^+]_e$ to 48–59 mM, $[Cl^-]_e$ to 70–75 mM, $[Ca^{++}]_e$ to 0.06–0.08 mM, and pH_e to 6.1–6.8; an accumulation of excitatory amino acids; a negative DC slow potential shift; and a decrease in ECS volume fraction to 0.04–0.07. The ECS volume starts to decrease when the blood pressure drops below 80 mm Hg and $[K^+]_e$ rises above 6 mM (Syková et al., 1994).

Figure 8 shows that during hypoxia and terminal anoxia, the ECS volume fraction in rat cortex or spinal cord decreases from 0.30 (note larger ECS volume in P8 rat) to 0.04, while tortuosity increases from 1.5 to about 2.2 (Lundbaek and Hansen, 1992; Syková et al., 1994). The same ultimate changes have been found in all neonatal, adult and aged rats, in grey and white matter, in the cortex, corpus callosum and spinal cord. However, the time course in white matter is significantly slower than in gray matter; and the time course in neonatal rats is about 10 times slower than in adults (Vořišek and Syková, 1997b). Linear regression analysis reveals a positive correlation between the normoxic size of the ECS volume and the time course of the changes. This corresponds to the well-known resistance of the immature CNS and the greater susceptibility of the aged brain to anoxia.

In recent studies using diffusion-weighted ^1H MRS/MRI, the apparent diffusion coefficient of water (ADC_W) was measured during terminal anoxia in rats. Anoxia evokes similar decreases in the apparent diffusion coefficient of ADC_W (measured by the NMR method) and ADC_{TMA} (measured by the TMA method). A comparison of the decreases in ADC_W and ADC_{TMA} in rats 8–9 days of age (P8–9) revealed the same time course, both corresponding to the decrease in ECS volume fraction (Fig. 8). Although water moves freely across the cellular membranes, TMA^+ stays predominantly in ECS. Since the total amount of tissue water is not believed to increase (Latour et al.,

1994; Van der Toorn et al., 1996), our study shows that changes in the *ADC* of brain tissue water measured by diffusion-weighted in vivo MR techniques reflect extra- and intracellular volume changes resulting from a water shift from the extra- to the intracellular compartment.

Full recovery to 'normoxic' diffusion parameters is achieved after successful recovery from severe ischemia (Lehmenkühler et al., 1993). Beginning 5–10 min after this recovery, the ECS volume fraction significantly increases above the 'normoxic' values to an α of about 0.30 (Table 2); λ and k' are not significantly different from the values found under normoxic conditions.

Diffusion parameters of the ECS in gliotic tissue

A stab wound of the rodent brain is a well-characterized and common model of reactive gliosis, which can impose diffusion barriers in the CNS due to the hypertrophy of astrocytic processes and an increased production of extracellular matrix

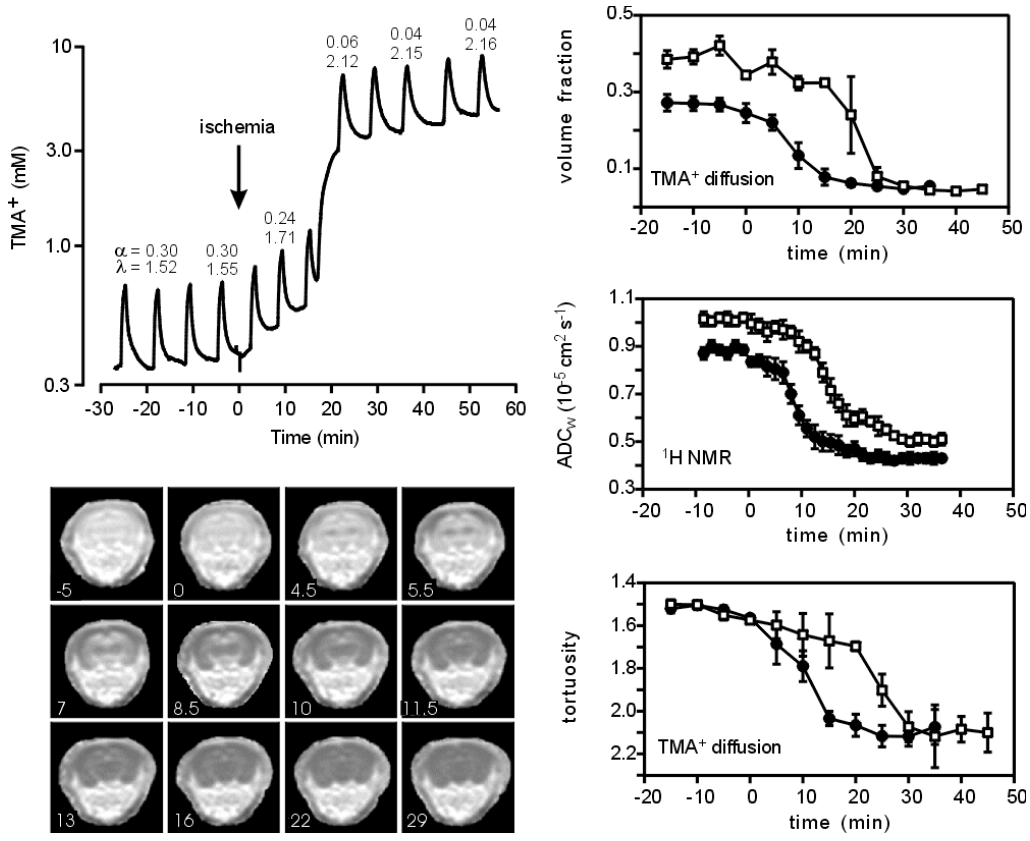

Fig. 8. Upper left: A typical TMA^+ diffusion experiment in the cortical gray matter (Layer V) of a 9-day-old rat. The TMA diffusion curves were recorded before and during global ischemia. The TMA^+ baseline increases and the superimposed diffusion curves show an increasing amplitude as ischemia progresses, because the scaling is logarithmic. The time after cardiac arrest and the α and λ values are shown with some curves. Below left: Water *ADC* maps of another 9-day-old rat brain before (–5) and at different times after cardiac arrest evoked by an i.p. injection of KCl (time after injection is shown with each record). The maps depict the calculated *ADC* on a pixel-by-pixel basis. The numbers in the lower left corner of the images indicate time. The *ADC* was calculated using diffusion-weighted NMR images obtained with U-FLARE (10 b values ranging up to 1500 s/mm^2) and fitting the intensities of the corresponding pixels in the images to the Stejskal-Tanner equation (see Van der Toon et al., 1996). Right: The time courses of *ADC* decrease, ECS volume decrease and tortuosity increase were found to be very similar (adapted from Van der Toorn et al., 1996).

components (Hatten et al., 1991; Norton et al., 1992; Ridet et al., 1997). We compared two different methods for revealing diffusion changes in rat cortex after injury: the TMA method and diffusion-weighted MR. The TMA and MR measurements were performed in the cortex of adult rats from the 3rd to the 35th day after a unilateral sterile cut through the cortex. Severe astrogliosis is found close to the injury site (up to 1 mm), and mild astrogliosis up to 2 mm from the wound in the ipsilateral cortex, but no astrogliosis is found in the auditory cortex or in the contralateral hemisphere. In contrast to GFAP staining, immunostaining for chondroitin-sulfate preoteoglycan increases in the whole ipsilateral hemisphere (Voříšek et al., 1999; Syková et al., 1999d). The mean values of α, ADC_{TMA} and ADC_W in the contralateral hemisphere were not significantly different from those in non-lesioned, control animals. In the astrogliotic cortex, less than 1 mm distant from the wound, the mean values of α are significantly higher ($\alpha = 0.26$), while the mean values of ADC_{TMA} are lower: (0.42×10^{-5} cm^2 s^{-1}). The more distant from the wound, the less the values of α and ADC_{TMA} differ from control values. On the other hand, ADC_W is significantly lower in the whole ipsilateral hemisphere, particularly in the auditory cortex: $ADC_W = (0.55 \times 10^{-5}$ cm^2 s^{-1}) (Fig. 9). We conclude that an increase in diffusion barriers, manifested by the decrease of both ADC_{TMA} and ADC_W, occurs throughout the entire cortex of the wounded hemisphere without significant changes in ECS volume. The changes are related to astrogliosis, particularly in and closely around the injured area, and to an increase in the extracellular matrix which occurs throughout the entire hemisphere.

These experiments revealed that not only glial swelling and astrogliosis, but also an increase in ECM content, are associated with a long-term increase of diffusion barriers in the ECS, and can, therefore, lead to the impairment of the diffusion of neuroactive substances and of volume transmission (Roitbak and Syková, 1999).

Extracellular space diffusion parameters during development

Compared to healthy adults, ECS diffusion parameters significantly differ during postnatal development (Lehmenkühler et al., 1993; Prokopová et al., 1997; Voříšek and Syková, 1997a; Voříšek and Syková, 1997b). The ECS volume in the cortex is about twice as large ($\alpha = 0.36$–0.46) in the newborn rat as in the adult rat ($\alpha = 0.21$–0.23), while the tortuosity increases with age (Table 2). The reduction in the ECS volume fraction correlates well with the growth of blood vessels. The larger ECS in the first days of postnatal development can be attributed to incomplete neuronal migration, gliogenesis and angiogenesis and to the presence of large extracellular matrix proteoglycans, particularly hyaluronic acid, which due to the mutual repulsion of its highly negatively charged branches occupies a great deal of space and holds cells apart. In rat spinal cord gray matter, α decreases with neuronal development and gliogenesis from postnatal day 4 to 12 by about 15%, while λ significantly increases, showing that the diffusion of molecules becomes more hindered with age. The large ECS channels during development may allow the migration of larger substances (e.g. growth factors) and provide better conditions for cell migration during development. On the other hand, the large ECS in the neonatal brain could significantly dilute ions, metabolites and neuroactive substances released from cells, relative to release in adults, and may be a factor in the prevention of anoxic injury, seizure and spreading depression in young individuals. The diffusion parameters could also play an important role in the developmental process itself; diffusion parameters are substantially different in myelinated and unmyelinated white matter (Prokopová et al., 1997; Voříšek and Syková, 1997a). Isotropic diffusion is found in the corpus callosum and spinal cord white matter of young rats with incomplete myelination. In myelinated spinal cord and corpus callosum, the tortuosity is higher (the apparent diffusion coefficient is lower) when TMA^+ diffuses across the axons than when it diffuses along the fibers (Fig. 4).

Diffusion properties of the nervous tissue after neonatal X-irradiation

The CNS during the early postnatal period is more sensitive to X-irradiation than is the adult nervous

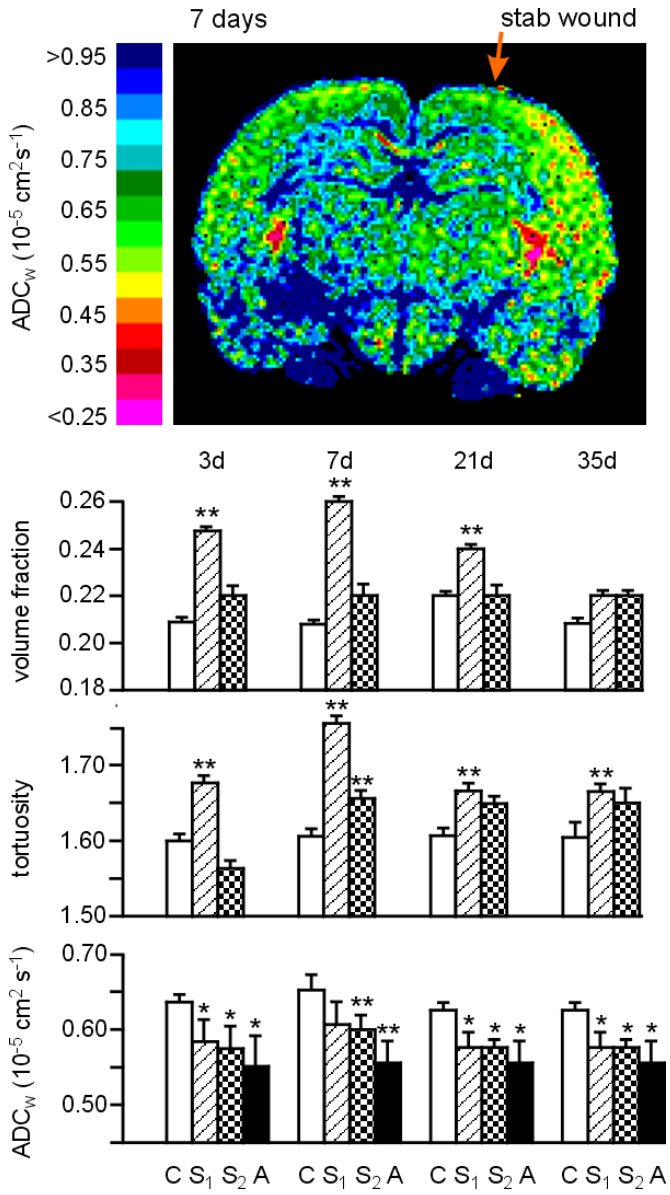

Fig. 9. ECS volume fraction, TMA tortuosity and ADC_w as measured by the TMA method and DW–NMR. The pseudocolour image shows the ADC_w map of a rat brain 7 days after a cortical stab wound. Note that ADC_w is lower in the entire cortex of the wounded hemisphere than in the contralateral hemisphere (C). The bar charts show the ECS volume fraction and tortuosity as measured by TMA method, and ADC_w as measured by DW–NMR. Data were obtained in the cortex of the injured and contralateral hemisphere 3, 7, 21 and 35 days post-lession (d). All data are expressed as mean ± SEM. The asterisks above columns indicate significant diference from the values in contralateral hemisphere, * = $p < 0.05$, ** = $p < 0.01$. The ECS volume fraction, as measured by the TMA method, revealed significant changes only in the vicinity of the wound in the area S1 (up to 1000 μm from the wound); tortuosity is increased in the area S1 as well as in S2 (1000–2000 μm from the wound). Significant changes in ADC_w were found in the entire ipsilateral hemisphere including the auditory cortex (A). This corresponded to an increase in chondroitin sulphate immunostaining (not shown).

system, apparently due to the proliferative potential and increased radiation sensitivity of glial and vascular endothelial cells in the immature nervous system. In experiments on the somatosensory neocortex and subcortical white matter of 1-day-old (P1) rats, X-irradiation at a single dose of 40 Gy results in radiation necrosis with typical early morphological changes in the tissue, namely cell death, DNA fragmentation, extensive neuronal loss, blood-brain-barrier (BBB) damage, activated macrophages, astrogliosis, an increase in extracellular fibronectin, and concomitant changes in all three diffusion parameters. The changes are observed as early as 48 hours post-irradiation and persist at P21 (Syková et al., 1996). Under normal conditions, the volume fraction of the ECS in the cortex is large in newborn rats, $\alpha = 0.35$–0.40, diminishes with age and reaches adult values at P21 (Lehmenkühler et al., 1993). X-irradiation at a single dose of 40 Gy blocks the normal pattern of volume fraction decrease during postnatal development and results in a significant increase in the ECS volume (Syková et al., 1996). The volume fraction in both cortex and corpus callosum increases to about 0.50. This increase persists at 3 weeks after X-irradiation. Tortuosity and non-specific uptake significantly decrease at 48 hours (P2); at P8–P9 they are not significantly different from those of control animals, and both significantly increase with astrogliosis at P10–P21. These data indicate that in chronic lesions, which occur 1–3 weeks after X-irradiation and/or in gliotic tissue, the volume fraction remains elevated, while tortuosity increases due to astrogliosis. Even when X-irradiation at a single dose of 20 Gy is used, resulting in relatively light neuronal damage and loss and BBB damage, it produces similar changes in diffusion parameters as those found with 40 Gy. Less pronounced but significant changes in diffusion parameters are also found in areas adjacent to the directly X-irradiated cortex of the ipsilateral hemisphere and in the contralateral hemisphere.

It is evident that the block of postnatal gliogenesis and the damage to neurons evoked by X-irradiation results in an even greater increase in the ECS volume fraction of nervous tissue than injury evoked by a stab wound. Thus it can substantially contribute to impaired signal transmission, e.g. by diluting ions and neuroactive substances released from cells, and may thus play an important role not only in functional deficits, but also in malfunctions during the developmental processes. Moreover, the increase in ECS volume and tortuosity in the X-irradiated cortex as well as in the contralateral hemisphere suggests that the diffusion of substances can be substantially changed even a long time after mild irradiation.

ECS volume and geometry during inflammation and demyelination

Changes in ECS diffusion parameters can be expected during inflammation, during which brain edema may develop; in an experimental model, inflammation was evoked by an intracerebral inoculation of a weakly pathogenic strain of *Staphylococcus aureus* (Lo et al., 1993). Acute inflammation and an increase in BBB permeability in the abscess region resulted in rather mild changes in the ECS diffusion parameters, i.e. the volume fraction tended to be somewhat larger and the tortuosity somewhat smaller.

Dramatic changes in the ECS diffusion parameters are found in the spinal cord of rats during experimental autoimmune encephalomyelitis (EAE), an experimental model of multiple sclerosis (Šimonová et al., 1996). EAE, which is induced by the injection of guinea-pig myelin basic protein (MBP), results in typical morphological changes in the CNS tissue, namely demyelination, an inflammatory reaction, astrogliosis, BBB damage and paraparesis, at 14–17 days post-injection. Paraparesis is accompanied by increases in α in the dorsal horn, in the intermediate region, in the ventral horn and in white matter from about 0.18 to about 0.30 (Table 2). The λ in the dorsal horn and the intermediate region significantly decreases and k' decreases in the intermediate region and the ventral horn (Šimonová et al., 1996). There is a close correlation between the changes in ECS diffusion parameters and the manifestation of neurological abnormalities.

These results suggest that the expansion of the ECS alters diffusion parameters in inflammatory and demyelinating diseases and may affect the accumulation and movement of ions, neurotran-

smitters, neuromodulators and metabolites in the CNS in these disorders, possibly by interfering with axonal conduction.

Diffusion properties of malignant tumors

Cancer is the second leading cause of death in many industrialized countries, and malignant brain tumors, particularly the gliomas, are among the deadliest of tumors, since many patients, including children, die within two years. Only recently have basic new findings about tumor cell division, differentiation and migration, the relationship between glial cells and gliomas, the existence of multiple glial precursor cell populations and new insights into the developmental biology of glial cells been made. One of the recently discussed issues is the existence of CNS-specific extracellular matrix proteins, e.g. brain-enriched hyaluronan binding proteins (BEHAB) and brevican, that are expressed at high levels during initial gliogenesis and also in all types and grades of human gliomas (Jaworski et al., 1996). Hyaluronan binding proteins help cells to move through tissue during development and have also been associated with invasive cancers. It has also been suggested that the migration of cells could be critically dependent on their shape and size, their binding to various proteins in the extracellular space (ECS) such as hyaluronan-binding protein that can boost the invasiveness of tumors, and on the size and geometry of the ECS. The delivery of drugs to tumors is affected by the permeability of the blood-brain-barrier, their diffusion through the ECS in normal and malignant tissue, and their side-effects on healthy cells surrounding the tumor. It is therefore crucial to quantify the size, composition and geometry of the extracellular space as these factors critically affect cell migration and the diffusion of substances in the brain (for review see Syková, 1997; Nicholson and Syková, 1998).

Older studies, particularly using sucrose space and electron microscopic methods, showed that the visible extracellular compartment is larger in brain tumors, particularly in gliomas, than in normal brain tissue (Bakay, 1970a, b). However, these methods resulted either in small values for the size of the extracellular space because of tissue shrinkage during fixation and embedding, or did not allow one to measure the absolute values of ECS size and geometry or to follow the diffusion of molecules of different sizes and shapes. Increased extracellular space, along with the above-mentioned extracellular matrix proteins, could allow cells to migrate more easily in tumors and into surrounding tissue. Shrinkage of the extracellular space and extracellular matrix proteins could slow or substantially limit the diffusion and migration of cells.

To quantify extracellular space size, geometry and diffusion properties in tumors (particularly malignant gliomas) TMA measurments were performed in slices from surgically removed pieces of patients' brains. We found that the more malignant the glioma, the more dramatic is the increase in the ECS volume. In many brain slices from glioblastomas (grade 4, WHO classification system), the ECS volume is as large as 37–46% of total tissue volume (Fig. 2). There is also an increase in tortuosity which can be due either to the frequently observed astrogliosis or to changes in the extracellular matrix. It is therefore reasonable to assume that the ECS composition, volume and geometry play an important role in cancer malignancy and invasiveness. The size of the ECS in malignant tumors and their geometry and structure should be considered during therapeutic drug delivery.

ECS diffusion parameters and aging

In the mammalian brain, higher cognitive functions such as learning and memory depend upon the circuits that run through the hippocampus. Until recently, learning deficits during aging have been associated with neuronal degeneration and synaptic inefficiency. However, recent observations of a lack of hippocampal cell loss in aged humans, monkeys and rats (West, 1993; Rapp and Gallagher, 1996; Rasmussen et al., 1996) suggest that age-related functional change in the nervous system may not necessarily be a sign of degenerative pathology. The question thus arises whether learning deficits during aging also involve the impairment of extrasynaptic or 'volume' transmission, i.e. the diffusion of neuroactive substances in the ECS.

The ECS diffusion parameters α, $\lambda_{x,y,z}$ and k' were measured in the cortex, corpus callosum and

hippocampus (CA1, CA3 and in dentate gyrus). If diffusion in a particular brain region is anisotropic, then the correct value of the ECS volume fraction cannot be calculated from measurements done only in one direction. For anisotropic diffusion, the diagonal components of the tortuosity tensor are not equal, and generally its non-diagonal components need not be zero. Neverthless, if a suitable frame of reference is chosen (i.e. if we measure in three privileged orthogonal directions), neglecting the non-diagonal components becomes possible, and the correct value of the ECS size can thus be determined (Rice et al., 1993; Mazel et al., 1998). Therefore, TMA^+ diffusion was measured in the ECS independently along three orthogonal axes (x – transversal, y – sagital, z – vertical). In all three regions – cortex, corpus callosum and hippocampus – the mean ECS volume fraction α was significantly lower in aged rats (26–32 months old), ranging from 0.17 to 0.19, than in young adults (3–4 months old) in which α ranged from 0.21 to 0.22 (Table 2). Non-specific uptake k' was also significantly lower in aged rats. Importantly, there is a loss of anisotropy in the aging hippocampus, particularly in the CA3 region and the dentate gyrus (Syková et al., 1998b).

The three-dimensional pattern of diffusion away from a point source can be illustrated by constructing iso-concentration spheres (isotropic diffusion) or ellipsoids (anisotropic diffusion) for extracellular TMA^+ concentration. The surfaces in Fig. 5 represent the locations where TMA^+ concentration first reached 1 mM, 60 sec after its application in the center. The ellipsoid in the hippocampus of the young adult rat reflects the different abilities of substances to diffuse along the x-, y- and z-axes, while the sphere in the hippocampus of the aged rat shows isotropic diffusion. The smaller ECS volume fraction in aged rats is reflected in the spheres being larger than the ellipsoid.

Morphological changes during aging include cell loss, loss of dendritic processes, demyelination, astrogliosis, swollen astrocytic processes and changes in the extracellular matrix. It is reasonable to assume that there is a significant decrease in the *ADC* of many neuroactive substances in the aging brain, which accompanies astrogliosis and changes in the extracellular matrix. One of the explanations of why α in the cortex, corpus callosum and hippocampus of senescent rats is significantly lower than in young adults could be astrogliosis in the aged brain. Increased GFAP staining and an increase in the size and fibrous character of astrocytes have been found in the cortex, corpus callosum and hippocampus of senescent rats, which may account for changes in the ECS volume fraction (Syková et al., 1998b). Other changes could account for the decreases in λ values and for the disruption of tissue anisotropy. In the hippocampus in CA1, CA3, as well as in the dentate gyrus, we have observed changes in the arrangement of fine astrocytic processes. These are normally organized in parallel in the x–y plane (Fig. 10A, B), and this organization totally disappears during aging. Moreover, the decreased staining for chondroitin sulfate proteoglycans and for fibronectin (Fig. 10C, D) suggests a loss of extracellular matrix macromolecules.

Because α is lower in aging rats, we expected some differences in the ECS diffusion parameter changes during ischemia in senescent rats. In fact, the final values of α, λ and k' induced by cardiac arrest are not significantly different between young and aged rats; however, the time course of all the changes is faster in aged animals (Syková et al., 1998b). The accelerated changes in extracellular space volume fraction and tortuosity evoked by ischemia in nervous tissue during aging can contribute to a more rapid impairment of signal transmission, e.g. due to a faster accumulation of ions and neuroactive substances released from cells and their slower diffusion away from the hypoxic/ischemic area in the more compacted ECS brought about by aging.

Our recent study also revealed that the degree of learning deficit during aging correlates with the changes in ECS volume, tortuosity and non-specific uptake (Syková et al., 1998a). The hippocampus is well-known for its role in memory formation, especially declarative memory. It is therefore reasonable to assume that diffusion anisotropy, which leads to a certain degree of specificity in extrasynaptic communication, may play an important role in memory formation. There was a significant difference between mildly and severely behaviorally impaired rats (rats were tested in a

Morris water maze), which was particularly apparent in the hippocampus. The ECS in the dentate gyrus of severely impaired rats was significantly smaller than in mildly impaired rats. Also, anisotropy in the hippocampus of severely impaired rats, particularly in the dentate gyrus, was much reduced, while a substantial degree of anisotropy was still present in aged rats with a better learning performance. Anisotropy might be important for extrasynaptic transmission by channeling the flux of substances in a preferential direction. Its loss may severely disrupt volume transmission in the CNS, which has been suggested to play an important role in memory formation (Syková et al., 1998a). Chodroitine sulphate proteoglycans participate in multiple cellular processes (Hardington and Fosang, 1992; Margolis and Margolis, 1993), including axonal outgrowth, axonal branching and synaptogenesis, which are important for the formation of memory traces.

What is the functional significance of the observed changes in ECS diffusion parameters during aging? We suggest that the alterations in hippocampal diffusion may account for the learning impairment seen in aged animals, either due to their effect on volume transmission (Nicholson and Syková, 1998) or on 'cross-talk' between synapses, which has been suggested to be involved in LTP and LTD (Kullmann et al., 1996; Kullmann, this volume), or on both. Anisotropy, which, particularly in the hippocampus and corpus callosum, may help to facilitate the diffusion of neuro-

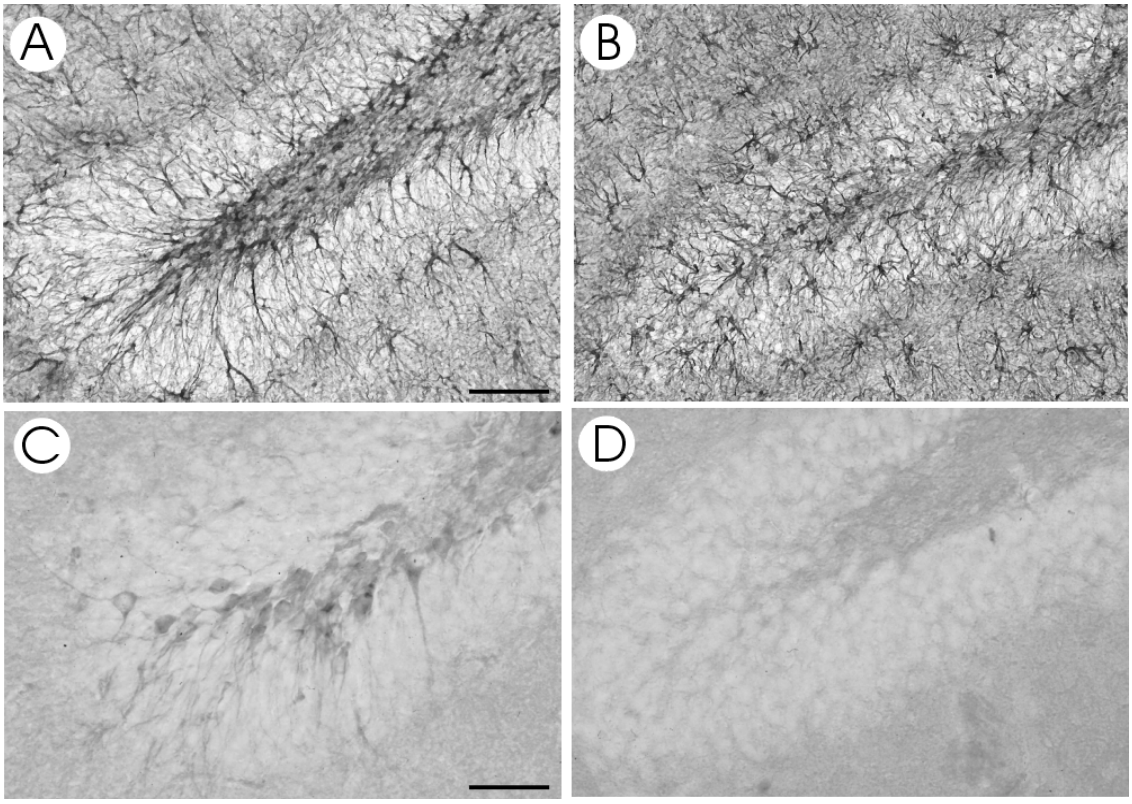

Fig. 10. Structural changes in the hippocampus gyrus dentatus region of aged rats. A: Astrocytes stained for GFAP in a young adult rat; note the radial organization of the astrocytic processes between the neurons (not stained). B: In an aged rat the radial organization of the astrocytic processes is lost. C: Staining for fibronectin in a young adult rat shows densely stained cells, apparently due to perineuronal staining around granular cells. D. In an aged rat the fibronectin staining is lost. Scale bar: in A and B = 100 μm, C and D = 50 μm. (From Syková et al., 1998b, by permission).

transmitters and neuromodulators to regions occupied by their high affinity extrasynaptical receptors, might have crucial importance for the specificity of signal transmission. The importance of anisotropy for the 'spill-over of glutamate', 'cross-talk' between synapses, and for LTP and LTD has been proposed (Kullmann et al., 1996; Asztely et al., 1997). The observed loss of anisotropy in senescent rats could therefore lead to impaired cortical and, particularly, hippocampal function. The decrease in ECS size could be responsible for the greater susceptibility of the aged brain to pathological events such as ischemia, cell death during anesthesia (Syková et al., 1998b), the poorer outcome of clinical therapy and the more limited recovery of affected tissue after insult.

Conclusions

There is increasing evidence that long-term changes in the physical and chemical parameters of the ECS accompany many physiological and pathological states. The 'acute' or relatively fast changes in the size of the intercellular channels are apparently a consequence of cellular (particularly glial) swelling. Abrupt ECS volume decrease may cause cellular or molecular 'crowding' (Zimmerman and Minton, 1993) which can lead to an acute increase in tortuosity. Long-term changes in diffusion would require changes in ECS composition, either permanent changes in the size of the intercellular channels, changes in extracellular matrix molecules, or changes in the number and thickness of cellular processes. Available data suggest that in some pathophysiological states α and λ behave as independent variables. A persistent increase in λ (without a decrease in ECS volume) is always found during astrogliosis and in myelinated tissue, suggesting that glial cells can form diffusion barriers, make the nervous tissue less permissive and play an important role in signal transmission, tissue regeneration and pathological states. This observation has important implications for our understanding of the function of glial cells. The extracellular matrix apparently also contributes to diffusion barriers and to diffusional anisotropy, particularly since its loss, e.g. during aging, correlates with a tortuosity decrease and a loss of anisotropy.

We may conlude that changes in ECS ionic composition, size and geometry may affect: (1) Synaptic transmission (width of synaptic clefts, permeability of ionic channels, concentration of transmitters, dendritic length constant, etc.), (2) Extrasynaptic 'volume' transmission by diffusion (diffusion of factors such as ions, NO, transmitters, neuropeptides, neurohormones, growth factors and metabolites), (3) Neuronal interaction and synchronization, (4) Neuron-glia communication, (5) ECS ionic homeostasis and glial function, (6) Clearance of metabolites and toxic products, (7) Permeability of ionic channels and (8) Regeneration processes. Long-term changes in local CNS architecture including ECS volume and tortuosity can apparently influence plastic changes, LTP or LTD, changes in behaviour and memory formation. Using the methods described in this chapter (not excluding possible new ones) will, in further studies, lead to a fuller understanding of the consequences that altered ECS size, content and geometry may have on nervous system function.

Acknowledgements

Supported by grants VS96–130, GA ČR 307/96/K226, GA ČR 309/97/K048, GA ČR 309/99/0657 and GA ČR 305/99/0655. We would like to thank Dr. M. Pekny and C. Eliasson for providing GFAP − / − mice.

List of abbreviations

ADC	apparent diffusion coefficient
CNS	central nervous system
ECM	extracellular matrix
ECS	extracellular space
GFAP	glial fibrillary acidic protein
HA	hyaluronic acid
HPMA	N-(2-hydroxypropyl)methacrylamide
IOI	integrative optical imaging
IOS	intrinsic optical signals
ISM	ion-selective microelectrode
LTD	long-term depression
LTP	long-term potentiation
NMR	nuclear magnetic resonance
PSA	polysialic acid
TEA	tetraethylammonium

TMA	tetramethylammonium
TW	total water content

References

Agnati, L.F., Zoli, M., Stromberg, I. and Fuxe, K. (1995) Intercellular communication in the brain: wiring versus volume transmission. *Neuroscience*, 69: 711–726.

Anděrová, M., Chvátal, A., Eliasson, C., Pěkný, M. and Syková, E. (1999) Membrane properties and swelling of astrocytes in GFAP–/– mice. *Physiol. Res.*, 48: S52.

Andrew, R.D. and MacVicar, B.A. (1994) Imaging cell volume changes and neuronal excitation in the hippocampal slice. *Neuroscience*, 62: 371–383.

Asztely, F., Erdemli, G. and Kullmann, D.M. (1997) Extrasynaptic glutamate spillover in the hippocampus: dependence on temperature and the role of active glutamate uptake. *Neuron*, 18: 281–293.

Bach-y-Rita, P. (1993) Neurotransmission in the brain by diffusion through the extracellular fluid: a review. *NeuroReport*, 4: 343–350.

Bakay, L. (1970a) The extracellular space in brain tumor. I. Morphological considerations. *Brain*, 93: 693–698.

Bakay, L. (1970b) The extracellular space in brain tumor. II. The sucrose space. *Brain*, 93: 699–707.

Becker, C.G., Artola, A., Gerardy-Schahn, R., Becker, T., Welzl, H. and Schachner, M. (1996) The polysialic acid modification of the neural cell adhesion molecule is involved in spatial learning and hippocampal long-term potentiation. *J. Neurosci. Res.*, 45: 143–152.

Benveniste, H., Hedlund, L.W. and Johnson, G.A. (1992) Mechanism of detection of acute cerebral ischemia in rats by diffusion-weighted magnetic resonance microscopy. *Stroke*, 23: 746–754.

Celio, M.R., Spreafico, R., De Biasi, S. and Vitellaro-Zuccarello, L. (1998) Perineuronal nets: past and present. *Trends Neurosci.*, 21: 510–515.

Chesler, M. (1990) The regulation and modulation of pH in the nervous system. *Prog. Neurobiol.*, 34: 401–427.

Cserr, H.F., De Pasquale, M., Nicholson, C., Patlak, C. Pettigrew, K.D. and Rice, M.E. (1991) Extracellular volume decreases while cell volume is maintained by ion uptake in rat brain during acute hypernatremia. *J. Physiol. (Lond.)*, 442: 277–295.

Dawson, H. and Segal, M.B. (1996) *Physiology of The CFS and Blood–Brain Barriers*. Boca Raton: CRC Press.

Deitmer, J.W. and Rose, C.R. (1996) pH regulation and proton signalling by glial cells. *Prog. Neurobiol.*, 48: 73–103.

Fuxe, K. and Agnati, L.F. (1991) *Volume Transmission in the Brain: Novel Mechanisms for Neural Transmission*. Raven Press, New York.

Hardington, T.E. and Fosang, A.J. (1992) Proteoglycans: many forms and many functions. *FASEB J.*, 6: 861–870.

Hatten, M.E., Liem, R.K. H., Shelanski, M.L. and Mason, C.A. (1991) Astroglia in CNS injury. *Glia*, 4: 233–243.

Jaworski, D.M., Kelly, G.M. and Hockfield, S. (1996) The CNS-specific hyaluronan binding protein, BEHAB, is expressed during periods of glial cell generation and motility. *Sem. Neurosci.*, 8: 391–396.

Jendelová, P. and Syková, E. (1991) Role of glia in K^+ and pH homeostasis in the neonatal rat spinal cord. *Glia*, 4: 56–63.

Johnston, B.M., Patuzzi, R., Syka, J. and Syková, E. (1989) Stimulus-related potassium changes in the organ of Corti of guinea pig. *J. Physiol. (Lond.)*, 408: 77–92.

Kimelberg, H.K. (1991) Swelling and volume control in brain astroglial cells. In: R. Gilles (Ed.), *Advances in Comparative and Environmental Physiology*, Springer-Verlag, Berlin, Heidelberg, pp. 81–117.

Kimelberg, H.K. and Ransom, B.R. (1986) Physiological and pathological aspects of astrocyte swelling. In: S. Federoff and A. Vernadakis (Eds), *Astrocytes: cell biology and pathology of astrocytes*, Academic Press, New York, pp. 129–166.

Kimelberg, H.K., Sankar, P., O'Connor, E.R., Jalonen, T. and Goderie, S.K. (1992) Functional consequences of astrocyte swelling. *Prog. Brain Res.*, 94: 57–68.

Korf, J., Klein, H.C. and Postrema, F. (1988) Increases in striatal and hippocampal impedance and extracellular levels of amino acids by cardiac arrest in freely moving rats. *J. Neurochem.*, 50: 1087–1096.

Križaj, D., Rice, M.E., Wardle, R.A. and Nicholson, C. (1996) Water compartmentalization and extracellular tortuosity after osmotic changes in cerebellum of *Trachemys scripta*. *J. Physiol. (Lond.)*, 492: 887–896.

Kullmann, D.M., Erdemli, G. and Asztely, F. (1996) LTP of AMPA and NMDA receptor-mediated signals: evidence for presynaptic expression and extrasynaptic glutamate spillover. *Neuron*, 17: 461–474.

Latour, L.L., Svoboda, K., Mitra, P.P. and Sotak, C.H. (1994) Time-dependent diffusion of water in a biological model system. *Proc. Natl Acad. Sci. USA*, 91: 1229–1233.

Le Bihan, D., Turner, R. and Douek, P. (1993) Is water diffusion restricted in human brain white matter? An echoplanar NMR imaging study. *NeuroReport*, 4: 887–890.

Lehmenkühler, A., Syková, E., Svoboda, J., Zilles, K. and Nicholson, C. (1993) Extracellular space parameters in the rat neocortex and subcortical white matter during postnatal development determined by diffusion analysis. *Neuroscience*, 55: 339–351.

Lo, W.D., Wolny, A.C., Timan, C., Shin, D. and Hinkle, G.H. (1993) Blood-brain barrier permeability and the brain extracellular space in acute cerebral inflammation. *J. Neurol. Sci.*, 118: 188–193.

Lundbaek, J.A. and Hansen, A.J. (1992) Brain interstitial volume fraction and tortuosity in anoxia. Evaluation of the ion-selective microelectrode method. *Acta Physiol. Scand.*, 146: 473–484.

Margolis, R.K. and Margolis, R.U. (1993) Nervous tissue proteoglycans. *Experientia*, 49: 429–446.

Matsuoka, Y. and Hossmann, K.A. (1982) Cortical impedance and extracellular volume changes following middle cerebral artery occlusion in cats. *J. Cereb. Blood Flow Metab.*, 2: 466–474.

Mazel, T. and Syková, E. (1999) Faster extracellular diffusion in the brain of GFAP–/– mice. *Physiol. Res.*, 48: S95.

Mazel, T., Šimonová, Z. and Syková, E. (1998) Diffusion heterogeneity and anisotropy in rat hippocampus. *NeuroReport*, 9: 1299–1304.

Moseley, M.E., Cohen, Y., Mintorovitch, J., Chileuitt, L., Shimizu, H., Kucharczyk, J., Wendland, M.F. and Weinstein, P.R. (1990) Early detection of regional cerebral ischemia in cats: comparison of diffusion- and T2-weighted MRI and spectroscopy. *Magn. Reson. Med.*, 14: 330–346.

Muller, D., Wang, C., Skibo, G., Toni, N., Cremer, H., Calaora, V., Rougon, G. and Kiss, J.Z. (1996) PSA-NCAM is required for activity-induced synaptic plasticity. *Neuron*, 17: 413–422.

Nicholson, C. (1979) Brain cell microenvironment as a communication channel. In: F.O. Schmitt and F.G. Worden (Eds), *The Neurosciences: Fourth Study Program*, Cambridge, MA: M.I.T. Press. pp. 457–476.

Nicholson, C. (1995) Interaction between diffusion and Michaelis–Menten uptake of dopamine after iontophoresis in striatum. *Biophys. J.*, 68: 1699–1715.

Nicholson, C. and Phillips, J.M. (1981) Ion diffusion modified by tortuosity and volume fraction in the extracellular microenvironment of the rat cerebellum. *J. Physiol. (Lond.)*, 321: 225–257.

Nicholson, C. and Syková, E. (1998) Extracellular space structure revealed by diffusion analysis. *Trends Neurosci.*, 21: 207–215.

Nicholson, C. and Tao, L. (1993) Hindered diffusion of high molecular weight compounds in brain extracellular microenvironment measured with integrative optical imaging. *Biophys. J.*, 65: 2277–2290.

Norris, D.G., Niendorf, T. and Leibfritz, D. (1994) Healthy and infarcted brain tissues studied at short diffusion times: the origins of apparent restriction and the reduction in apparent diffusion coefficient. *NMR in Biomed.*, 7: 304–310.

Norton, W.T., Aquino, D.A., Hosumi, I., Chiu, F.C. and Brosnan, C.F. (1992) Quantitative aspects of reactive gliosis: a review. *Neurochem. Res.*, 17: 877–885.

Pekny, M., Leveen, P., Pekna, M., Eliasson, C., Berthold, C.H., Westermark, B. and Betsholtz, C. (1995) Mice lacking glial fibrillary acidic protein display astrocytes devoid of intermediate filaments but develop and reproduce normally. *EMBO J.*, 14: 1590–1598.

Pérez-Pinzón, M.A., Tao, L. and Nicholson, C. (1995) Extraceullular potassium, volume fraction, and tortuosity in rat hippocampal CA1, CA3 and cortical slices during ischemia. *J. Neurophysiol.*, 74: 565–573.

Prokopová-Kubinová, S. and Syková, E. (in press) Extracellular diffusion parameters in spinal cord and filum terminale of the frog. *J. Neurosci. Res.*

Prokopová, Š., Nicholson, C. and Syková, E. (1996) The effect of 40-kDa or 70-kDa dextran and hyaluronic acid solution on extracelluar space tortuosity in isolated rat spinal cord. *Physiol. Res.*, 45: P28.

Prokopová, Š., Vargová, L. and Syková, E. (1997) Heterogeneous and anisotropic diffusion in the developing rat spinal cord. *NeuroReport*, 8: 3527–3532.

Prokopová, Š., Anděrová, M., Chvátal, A., Elliasson, C., Pekny, M. and Syková, E. (1998) Extracellular space diffusion parameters and membrane properties of astrocytes in GFAP-deficient mice. *Soc. Neurosci. Abstr.*, 24: 56.

Prokopová, Š., Vargová, L., Tao, L., Ulbrich, K., Šubr, V., Nicholson, C. and Syková, E. (1999) Diffusion of polymeric drug carriers in rat cortical slices measured by integrative optical imaging. *Physiol. Res.*, 48: S109.

Rapp, P.R. and Gallagher, M. (1996) Preserved neuron number in the hippocampus of aged rats with spatial learning deficits. *Proc. Natl Acad. Sci. USA*, 93: 9926–9930.

Rasmussen, T., Schliemann, T., Sorensen, J.C., Zimmer, J. and West, M.J. (1996) Memory impaired aged rats: no loss of principal hippocampal and subicular neurons. *Neurobiol. Aging*, 17: 143–147.

Rice, M.E. (2000) Ascorbate regulation and neuroprotective role in the brain. *Trends Neurosci.*, 23: 209–216.

Rice, M.E. and Nicholson, C. (1991) Diffusion characteristics and extracellular volume fraction during normoxia and hypoxia in slices of rat neostriatum. *J. Neurophysiol.*, 65: 264–272.

Rice, M.E., Okada, Y.C. and Nicholson, C. (1993) Anisotropic and heterogeneous diffusion in the turtle cerebellum: Implications for volume transmission. *J. Neurophysiol.*, 70: 2035–2044.

Richter, F., Vargová, L., Mazel, T. and Syková, E. (1999) Extracellular space size and geometry during and after cortical spreading depression in immature and adult rats. *Physiol. Res.*, 48: S112.

Ridet, J.I., Malhotra, S.K., Privat, A. and Gage, F.H. (1997) Reactive astrocytes: cellular and molecular cues to biological function. *Trends Neurosci.*, 20: 570–577.

Roitbak, T. and Syková, E. (1999) Diffusion barriers evoked in the rat cortex by reactive astrogliosis. *Glia*, 28: 40–48.

Šimonová, Z., Svoboda, J., Orkand, R., Bernard, C.C.A., Lassmann, H. and Syková, E. (1996) Changes of extracellular space volume and tortuosity in the spinal cord of Lewis rats with experimental autoimmune encephalomyelitis. *Physiol. Res.*, 45: 11–22.

Singer, W. and Lux, H.D. (1975) Extracellular potassium gradients and visual receptive fields in the cat striate cortex. *Brain Res.*, 96: 378–383.

Svoboda, J. and Syková, E. (1991) Extracellular space volume changes in the rat spinal cord produced by nerve stimulation and peripheral injury. *Brain Res.*, 560: 216–224.

Svoboda, J., Motin, V.G., Hájek, I. and Syková, E. (1988) Increase in extracellular potassium level in rat spinal dorsal horn induced by noxious stimulation and peripheral injury. *Brain Res.*, 458: 97–105.

Syková, E. (1983) Extracellular K^+ accumulation in the central nervous system. *Prog. Biophysiol. Molec. Biol.*, 42: 135–189.

Syková, E. (1987) Modulation of spinal cord transmission by changes in extracellular K^+ activity and extracellular volume. *Can. J. Physiol. Pharmacol.*, 65: 1058–1066.

Syková, E. (1992) *Ionic and volume changes in the microenvironment of nerve and receptor cells*. Springer-Verlag, Heidelberg.

Syková, E. (1997) The extracellular space in the CNS: Its regulation, volume and geometry in normal and pathological neuronal function. *Neuroscientist*, 3: 28–41.

Syková, E. and Svoboda, J. (1990) Extracellular alkaline-acid-alkaline transients in the rat spinal cord evoked by peripheral stimulation. *Brain Res.*, 512: 181–189.

Syková, E., Rothenberg, S. and Krekule, I. (1974) Changes of extracellular potassium concentration during spontaneous activity in the mesencephalic reticular formation of the rat. *Brain Res.*, 79: 333–337.

Syková, E., Kříž, N. and Preis, P. (1983) Elevated extracellular potassium concentration in unstimulated spinal dorsal horns of frogs. *Neurosci. Lett.*, 43: 293–298.

Syková, E., Jendelová, P., Svoboda, J., Sedman,G. and Ng, K.T. (1990) Activity-related rise in extracellular potassium concentration in the brain of 1–3-day-old chicks. *Brain Res. Bull.*, 24: 569–575.

Syková, E., Svoboda, J., Polák, J. and Chvátal, A. (1994) Extracellular volume fraction and diffusion characteristics during progressive ischemia and terminal anoxia in the spinal cord of the rat. *J. Cereb. Blood Flow Metab.*, 14: 301–311.

Syková, E., Svoboda, J., Šimonová, Z., Lehmenkühler, A. and Lassmann, H. (1996) X-irradiation-induced changes in the diffusion parameters of the developing rat brain. *Neuroscience*, 70: 597–612.

Syková, E., Mazel, T., Frisch, C., Šimonová, Z., Hasenöhrl, R.U. and Huston, J.P. (1998a) Spatial memory and diffusion parameters in aged rat cortex, corpus callosum and hippocampus. *Soc. Neurosci. Abstr.*, 24: 1420.

Syková, E., Mazel, T. and Šimonová, Z. (1998b) Diffusion constraints and neuron-glia interaction during aging. *Exp. Gerontol.*, 33: 837–851.

Syková, E., Mazel, T., Roitbak, T. and Šimonová, Z. (1999a) Morphological changes and diffusion barriers in auditory cortex and hippocampus of aged rats. *Assoc. Res. Otolaryngol. Abs.*, 22: 17.

Syková, E., Roitbak, T., Mazel, T., Šimonová, Z. and Harvey, A.R. (1999b) Astrocytes, oligodendroglia, extracellular space volume and geometry in rat fetal brain grafts. *Neuroscience*, 91: 783–798.

Syková, E., Vargová, L., Prokopová, Š. and Šimonová, Z. (1999c) Glial swelling and astrogliosis produce diffusion barriers in the rat spinal cord. *Glia*, 25: 56–70.

Syková, E., Vořišek, I., Tintěra, J., Roitbak, T. and Nicolay, K. (1999d) Water ADC, extracellular space volume and tortuosity in a rat model of injury. *Soc. Neurosci. Abstr.*, 25: 2064.

Tao, L. and Nicholson, C. (1996) Diffusion of albumins in rat cortical slices and relevance to volume transmission. *Neuroscience*, 75: 839–847.

Tao, L., Vořišek, I., Lehmenkühler, A., Syková, E. and Nicholson, C. (1995) Comparison of extracellular tortuosity derived from diffusion of 3 kDa dextran and TMA+ in rat cortical slices. *Soc. Neurosci. Abstr.*, 21: 604.

Thomas, L.B. and Steindler, D.A. (1995) Glial boundaries and scars: programs for normal development and wound healing in the brain. *Neuroscientist*, 1: 142–154.

Van der Toorn, A., Syková, E., Dijkhuizen, R.M., Vořišek, I., Vargová, L., Škobisová, E., Van Lookeren Campagne, M., Reese, T. and Nicolay, K. (1996) Dynamic changes in water ADC, energy metabolism, extracellular space volume, and tortuosity in neonatal rat brain during global ischemia. *Magn. Reson. Med.*, 36: 52–60.

Van Harreveld, A., Dafny, N. and Khattab, F.I. (1971) Effects of calcium on electrical resistance and the extracellular space of cerebral cortex. *Exp. Neurol.*, 31: 358–367.

Vargová, L., Tao, L., Syková, E., Ulbrich, K., Šubr, V. and Nicholson, C. (1998) Diffusion of large polymers in rat cortical slices measured by integrative optical imaging. *J. Physiol. (Lond.)*, 511: 16P.

Vargová, L., Prokopová, Š., Chvátal, A. and Syková, E. (1999) Are the changes in intrinsic optical signals a tool to measure changes in extracellular space volume? *Soc. Neurosci. Abstr.*, 25: 741.

Vořišek, I. and Syková, E. (1997a) Evolution of anisotropic diffusion in the developing rat corpus callosum. *J. Neurophysiol.*, 78: 912–919.

Vořišek, I. and Syková, E. (1997b) Ischemia-induced changes in the extracellular space diffusion parameters, K^+ and pH in the developing rat cortex and corpus callosum. *J. Cereb. Blood Flow Metab.*, 17: 191–203.

Vořišek, I., Roitbak, T., Nicolay, K. and Syková, E. (1999) Water ADC, extracellular space volume and tortuosity in the rat cortex during astrogliosis. *Physiol. Res.*, 48: S136.

Walz, W. (1989) Role of glial cells in the regulation of the brain ion microenvironment. *Prog. Neurobiol.*, 33: 309–333.

West, M.J. (1993) Regionally specific loss of neurons in the aging human hippocampus. *Neurobiol. Aging*, 14: 287–293.

Xie, Y., Zacharias, E., Hoff, P. and Tegtmeier, F. (1995) Ion channel involvment in anoxic depolarisation indused by cardiac arrest in rat brain. *J. Cereb. Blood Flow Metab.*, 15: 587–594.

Yang, P., Yin, X. and Rutishauser, U. (1992) Intercellular space is affected by the polysialic acid content of NCAM. *J. Cell Biol.*, 116: 1487–1496.

Zimmermann, S.B. and Minton, A.P. (1993) Macromolecular crowding: Biochemical, biophysical and physiological consequences. *Annu. Rev. Biophys. Biomol. Struct.*, 22: 27–65.

Zoli, M., Jansson, A., Syková, E., Agnati, L.F. and Fuxe, K. (1999) Intercellular communication in the central nervous system. The emergence of the volume transmission concept and its relevance for neuropsychopharmacology. *Trends Pharmacol. Sci.*, 20: 142–150.